

# **CERTIFICATION OF APPROVAL**

## **A SIMULATION APPROACH TO MODEL THE RESONANT FREQUENCIES AND THE RADIATION Q-FACTORS FOR A CYLINDRICAL DIELECTRIC RESONATOR ANTENNA**

by

Muhammad Kamil Hanis bin Hassan

A project dissertation submitted to the  
Department of Electrical & Electronic Engineering  
Universiti Teknologi PETRONAS  
in partial fulfilment of the requirement for the  
Bachelor of Engineering (Hons)  
(Electrical & Electronic Engineering)

Approved:

---

Dr Zuhairi Baharudin  
Project Supervisor

UNIVERSITI TEKNOLOGI PETRONAS  
TRONOH, PERAK

May 2012

## **CERTIFICATION OF ORIGINALITY**

This is to certify that I am responsible for the work submitted in this project, that the original work is my own except as specified in the references and acknowledgement, and that the original work contained herein have not been undertaken or done by unspecified sources or persons.

---

Muhammad Kamil Hanis bin Hassan

## **ACKNOWLEDGEMENT**

First of all, I would like to convey my highest gratitude to my Final Year Project Supervisor, Dr. Zuhairi bin Baharudin for his continuous support, knowledge, and words that kept me moving to complete this research project. And also, not forget to mention my Co – Supervisor of my Final Year Project, Mr. Mohd. Azman bin Zakariya for his continuous guidance and moral support.

I also would like to thank the Communication Lab Technologist; Mr. Adz Jamros bin Jamali for his willingness to provide me CST software and Agilent software. He taught me how to use CST software and Agilent software. He always gives me a hand whenever I need him.

Special thanks to Post Graduate Communication students, Mr. Muzammil and Mr. Affan for their efforts to teach me the basic of DRA. They helped me to understand more about my project.

Finally, thanks to my very own Universiti Teknologi PETRONAS, for the facilities, laboratories and consumables given to me.

## ABSTRACT

Modeling is the foundation to design the dielectric resonator antenna by following our own specifications. Since it is very important, this project will discover the modeling of the resonant frequency and the radiation Q factor for a cylindrical dielectric resonator antenna. There are two types coupling that will be implemented in this project which microstrip line coupling and coplanar waveguide coupling. As for microstrip line coupling, the material of Cylindrical Dielectric Resonator Antenna (CDRA) been use is carbon and for coplanar waveguide coupling is CCTO ( $\text{CaCu}_3\text{Ti}_4\text{O}_{12}$ ). A thin layer of metal will be placed on the top of CDRA for both coupling. The designing process accomplished by using Computer Simulation Technology (CST) software. Agilent software will be involved in the analysis stage. The modeling process involved by using the result of the return loss of the simulation. Microsoft Excel will be used to record and plot the data of the return loss. By using the plotted graph, the curve fitting method will be used to generate the general equation of polynomial expression. Based on the polynomial expression, the value of the parameters will be altered in order to obtain the model that as close as the result of the simulated return loss. The 6<sup>th</sup> order polynomial has been chosen to be the model since it produces very accurate result.

## TABLE OF CONTENTS

LIST OF TABLES .....	ix
LIST OF FIGURES .....	x
CHAPTER 1 INTRODUCTION .....	12
1.1 Background of Study.....	12
1.2 Problem Statement .....	13
1.2.1 Problem Identification .....	13
1.2.2 Significant of Project .....	13
1.3 Objective & Scope of Project.....	13
1.3.1 Main Objective .....	13
1.3.2 Scope of Project.....	14
1.4 Relevancy of Project .....	14
1.5 Feasibility of Project .....	14
CHAPTER 2 LITERATURE REVIEW .....	15
2.1 Introduction of Antenna .....	15
2.1.1 Antenna Basic.....	15
2.1.1.1 Aperture.....	15
2.1.1.2 Gain .....	15
2.1.1.3 Reciprocity .....	16
2.1.1.4 Directivity and Beam width .....	16
2.1.1.5 Side lobes .....	16
2.1.1.6 E-plane and H-plane.....	17
2.1.1.7 Path Loss .....	17
2.2 Dielectric Resonator Antenna (DRA) .....	17
2.3 Characteristics of DRA .....	19
2.4 Shapes of DRAs .....	20
2.4.1 Hemispherical Dielectric Resonator Antenna.....	20
2.4.1.1 Field Mode Configurations of Hemispherical DRA .....	21
2.4.2 Cylindrical Dielectric Resonator Antenna.....	23
2.4.2.1 Field Mode Configurations of Cylindrical DRA.....	23
2.4.3 Rectangular Dielectric Resonator Antenna .....	26
2.4.3.1 Field Mode Configurations of Rectangular DRA .....	27

2.5 Coupling to DRAs .....	28
2.5.1 Aperture Coupling .....	28
2.5.2 Probe Coupling .....	31
2.5.3 Microstrip Line Coupling .....	32
2.5.4 Coplanar Coupling.....	32
2.5.5 Dielectric Image Guide Coupling.....	34
CHAPTER 3 METHODOLOGY .....	35
3.1 Research Methodology.....	35
3.2 Flow Chart.....	36
3.2.1 Description of Flow Chart .....	37
3.2.1.1 Literature review .....	37
3.2.1.2 Design the CDRA using CST.....	37
3.2.1.3 Simulate the designed CDRA using CST .....	39
3.2.1.4 Analyzed the CDRA's result using Microsoft Excel and Agilent software .....	39
3.2.1.5 Use curve fitting approach method to obtain the modeling	39
3.2.1.6 Model validation and testing .....	39
3.3 Gantt chart and Milestone for Final Year Project I.....	40
3.3.1 Gantt chart for Final Year Project I.....	40
3.3.2 Milestone for Final Year Project I.....	41
3.4 Gantt chart for Final Year Project II .....	42
3.4.1 Gantt chart .....	42
3.4.2 Milestone for Final Year Project II.....	42
3.5 Tools.....	43
3.6 Project Schedule.....	43
CHAPTER 4 RESULT AND DISCUSSIONS .....	44
4.1 Cylindrical Dielectric Resonator Antenna with Microstrip Coupling .....	44
4.1.1 Antenna Structure .....	44
4.1.1.1 Result of the CDRA with microstrip coupling.....	47
4.2 Cylindrical Dielectric Resonator Antenna with Coplanar Waveguide Coupling.....	59
4.2.1 Antenna Structure .....	59
4.2.1.1 Result of the CDRA with Coplanar Waveguide coupling .	60
CHAPTER 5 CONCLUSION AND RECOMMENDATIONS .....	67

5.1 Conclusion.....	67
5.2 Recommendation.....	67
References .....	69

## LIST OF TABLES

Table 1 : Milestone for Final Year Project I.....	41
Table 2 : Milestone for Final Year Project II.....	42
Table 3 : Project schedule for Final Year Project I.....	43
Table 4 : Project schedule for Final Year Project II.....	43
Table 5 : Results of Simulated Return Loss at 2.45 GHz .....	50
Table 6 : Results of Simulated Return Loss at 2.45 GHz .....	51
Table 7 : Results of Simulated Return Loss at 2.45 GHz .....	52
Table 8 : Results of Simulated Return Loss at 2.45 GHz .....	53
Table 9 : Results of Simulated Return Loss at 2.45 GHz .....	54
Table 10 : Recorded data from the return loss of the CDRA.....	55
Table 11 : Analysis of modeling for Microstrip .....	58
Table 12 : Results of Simulated Return Loss at 2.45 GHz .....	62
Table 13 : Recorded data from the return loss of the CDRA.....	63
Table 14 : Analysis of modeling for Coplanar Waveguide .....	66



## LIST OF FIGURES

Figure 1 : Typical Antenna Pattern with Sidelobes .....	16
Figure 2 : DRA fed with coaxial probe and attach to ground plane .....	18
Figure 3 : Example of Hemispherical DRA shape.....	20
Figure 4 : Ideal radiation models of the dielectric resonator antenna on an infinite ground plane .....	21
Figure 5 : Geometry of the cylindrical DRA .....	23
Figure 6 : $koa$ of the $HE_{11\delta}$ mode of the cylindrical DRA.....	25
Figure 7 : Q-factor of the $HE_{11\delta}$ mode of the cylindrical DRA.....	26
Figure 8 : Geometry for rectangular DRA .....	27
Figure 9 : Various slot apertures.....	29
Figure 10 : Slot aperture coupling to a rectangular DRA .....	29
Figure 11 : Slot aperture coupling to a cylindrical DRA .....	30
Figure 12 : Slot aperture coupling to a split-cylindrical DRA.....	30
Figure 13 : Vertical probe sources .....	31
Figure 14 : Microstrip line coupling to DRAs .....	32
Figure 15 : Various coplanar feeds for coupling to DRAs.....	33
Figure 16 : Coplanar loop coupling to a cylindrical DRA.....	33
Figure 17 : Dielectric image guide feed for DRAs .....	34
Figure 18 : Flow chart of designing and modeling a CDRA .....	36
Figure 19 : Gantt chart for Final Year Project I.....	40
Figure 20 : Gantt chart for Final Year Project II.....	42
Figure 21 : Front view of CDRA with microstrip coupling designed using CST .....	45
Figure 22 : Back view of CDRA with microstrip coupling designed using CST .....	45
Figure 23 : The signal indication for signal strength (refer to the color only).....	46
Figure 24 : Return Loss of the CDRA with microstrip coupling.....	47
Figure 25 : Gain of the CDRA with microstrip coupling.....	48
Figure 26 : Directivity of the CDRA with microstrip coupling.....	48
Figure 27 : Legends that refers to the size of slot expansion.....	49
Figure 28 : Return loss when the slot at 39 mm from top.....	49
Figure 29 : The equivalent circuit when slot at 39 mm from top.....	49
Figure 30 : Return loss when the slot at 40 mm from top.....	50
Figure 31 : The equivalent circuit when slot at 40 mm from top.....	50

Figure 32 : Return loss when the slot at 41 mm from top.....	51
Figure 33 : The equivalent circuit when slot at 41 mm from top.....	51
Figure 34 : Return loss when the slot at 42 mm from top.....	52
Figure 35 : The equivalent circuit when slot at 42 mm from top.....	53
Figure 36 : Return loss when the slot at 43 mm from top.....	53
Figure 37 : The equivalent circuit when slot at 43 mm from top.....	54
Figure 38 : Plotted graph of CDRA by using Microsoft Excel.....	57
Figure 39 : Front view of the DRA with coplanar waveguide feeding using CST .....	59
Figure 40 : Return loss of the CDRA.....	60
Figure 41 : Gain of the CDRA .....	61
Figure 42 : Directivity of the CDRA.....	61
Figure 43 : Return loss when the CDRA positioned from 39 mm to 42 mm from top .....	62
Figure 44 : The equivalent circuit when slot at 39 mm from top.....	62
Figure 45 : Plotted graph of CDRA by using Microsoft Excel.....	65

# CHAPTER 1

## INTRODUCTION

### 1.1 Background of Study

The history of Dielectric Resonator Antenna (DRA) started in 1939 by Richtinger [1][2]. He was the first researcher that tested the microwave resonators in the form of non-metallized dielectric in the shape of toroid and sphere theoretically. Early 1960's, those modes of the non-metallized dielectric were analyzed by Okaya and Barash [3]. The dielectric resonators are enclosed in metal cavities to prevent any radiation. The shield is used to maintain the high quality factor. DRA have shown themselves as an ideal alternative for antenna application by offer several advantages including large impedance bandwidth [4], mechanical simplicity, and also for simple coupling schemes to all transmission line [5][6], provide high radiation efficiency, more resilient to the nearness detuning when placed close to any other object. The size of the DRA is smaller compared to the other conventional antennas. It can also be varied by choosing the dielectric constant of the resonator material and its own dimensions [7][8]. It has been preferred to replace the traditional low-gain antenna because it is easy to fabricate and also offer more degree of freedom in order to control the resonant frequency and Q factor. Nevertheless, high Q- factor will limit the bandwidth, thus will limit its usefulness and characteristics as an antenna.

The objective of this project is to design, simulate and modeling the cylindrical dielectric resonator antenna (CDRA). The modes of an isolated CDRA can be divided into three types which are transverse electric (TE) mode, transverse magnetic (TM) mode and hybrid (HE) mode. This project will use the HE mode to analyze the results of the simulation.

## 1.2 Problem Statement

### 1.2.1 Problem Identification

We lived in a rapid development progression of wireless microwave system technology that demands on high performance, low power consumption communication units particularly for portable devices. This project proposes the equation modeling on CDRA. Modeling will help to explain a system and to learn the effect of parameter of other components and to make predictions about behavior of the system [9]. There is no specific modeling for a CDRA so far. So, by obtained the CDRA modeling, it will helps engineer to design a new CDRA by using their own desired dielectric constant,  $\epsilon_r$ , and also help them to understand more about the design characteristics. Without modeling, it is hard to understand the behavior of the CDRA.

### 1.2.2 Significant of Project

By having some specific numerical modeling, it will help engineers and researchers to design their own CDRA that will meet their specifications. It will help the engineers to develop the CDRA for various applications. Thus, it will also help others to understanding better about the performance and characteristics of the CDRA.

## 1.3 Objective & Scope of Project

### 1.3.1 Main Objective

- To obtain the mathematical modeling that can represent the CDRA with different slot size and different positioning of the slot by using microstrip line feeding technique.
- To analyze the resonant frequency and Q factors for different feeding techniques that is microstrip line and coplanar waveguide.
- To obtain the mathematical modeling that can represent CDRA by using coplanar waveguide coupling technique.

### 1.3.2 Scope of Project

This project will start with literature review that related to the DRA and CDRA. The designed and the simulation will be done by using Computer Simulation Technology (CST) Microwave Studio software. And further results from the simulation will be analyzed by using Agilent software. Microsoft Excel will be used to record the data of the return loss of the CDRA. The data will be used to plot the graph of return loss. By using curve fitting method, the general form of polynomial equation will be generated.

### 1.4 Relevancy of Project

Since there is no modeling about the CDRA design, so this project will help the engineers to design the CDRA easily and gain the understanding about the characteristics of the CDRA's modes. Another aspect is to help engineers to design the CDRA based on the desired dielectric material.

### 1.5 Feasibility of Project

This project will be done in two semesters which include research, designing, simulation, analyzing and modeling of the CDRA. The main objective of this project is to determine the mathematical modeling for the CDRA's modes. For research part, all the information about the CDRA has been gathered from journals, books and conference proceedings. CST Microwave Studio will be used as tool to design and simulate the designed CDRA. Results that obtained from the CST Microwave Studio will be interpreted. Agilent software will be used to analyze the simulation results and Microsoft Excel will be used to develop the modeling.

## **CHAPTER 2**

### **LITERATURE REVIEW**

#### 2.1 Introduction of Antenna

Antenna gain is important for microwave communication. Antenna helps transmitting and receiving signal. It also provides high gain within the range of fabrication skills and budgets. Horns, lenses and dishes are the three types of antenna that meet those criteria above. Horns are foolproof, easy to build and simple. For a 10 GHz resonant frequency, horn antenna with 17 dB gain will fit in the palm of a hand. Metal-plate lenses are light in weight, non-critical to adjust and easy to build [10]. Dishes will provide very high gain. For a 2-foot dish antenna at 10 GHz resonant frequency, produce gain that more than 30 dB.

##### 2.1.1 Antenna Basic

As stated earlier, antenna is important device for radio communication. Below are some of the antenna basics:

###### 2.1.1.1 Aperture

This is where the area of an antenna captures energy from any passing radio wave [11].

###### 2.1.1.2 Gain

Theoretically, this is a point source of an antenna that radiates its energy or wave in all directions equally. Practically, antenna will radiate the energy to some direction compared to the other direction, which means it will make the antenna is directional antenna or omnidirectional antenna. In order to determine the gain of antenna, it will be focus on maximum gain only. That is when the antenna radiates maximum energy in some particular direction compared to the other direction. Use equation below to calculate gain in dBi:

$$G_{\text{dBi}} = 10 \log_{10} \left( \eta \frac{4\pi}{\lambda^2} A \right) \quad (1)$$

$\eta$ , is the represent the efficiency of antenna.

### 2.1.1.3 Reciprocity

Transmitting and receiving gains of antenna and antenna pattern are identical [11]. With identical antenna gains, the relative noise that received by different types of antennas will be different.

### 2.1.1.4 Directivity and Beam width

The bigger antenna's gain thus the smaller the antenna's bandwidth. Directivity of an antenna is measured by compared its maximum gain at particular direction with the averaged gain in all direction.

### 2.1.1.5 Side lobes

In real world, there is no antenna that able to radiate its energy to one direction only. In the radiated energy, there will be peaks and valleys as shown in Figure 1 below. The peaks are denoted to side lobes, down from the preferred direction or main lobe.

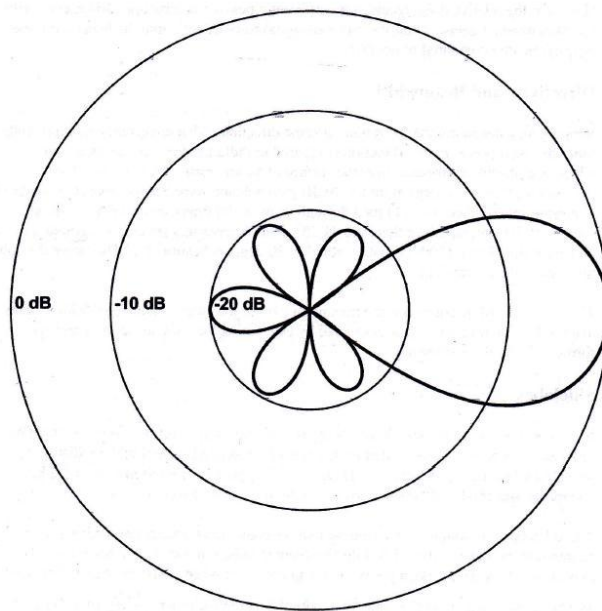


Figure 1 : Typical Antenna Pattern with Sidelobes

### 2.1.1.6 E-plane and H-plane

Electromagnetic field consists of an electric field and magnetic field that travelling at right angle to each other which later converts current and voltage on a transmission line into an electromagnetic field in space. A dipole provides electric field, by creating a pattern with larger amplitude in planes which include the dipole. The electric field travel in E-plane while magnetic field travel in H-plane. H-plane is perpendicular to E-plane. In polarization of antenna, we must refer the E-plane. In order to fully utilize and achieve maximum gain for three dimensional antennas, it is important to consider both E and H-plane.

### 2.1.1.7 Path Loss

The Friis transmission loss equation used to estimate the path loss between two antennas, a transmitting antenna,  $G_T$ , and a receiving antenna,  $G_R$ . The Friis equation as below:

$$G_R \text{ Loss(dB)} = 10. \log \left( \frac{4\pi d}{\lambda} \right)^2 - G_T(\text{dBi}) - G_R(\text{dBi}) \quad (2)$$

Where,

$d$  is the distance between the two antennas,

$G_T$  is transmitting gain,

$G_R$  is the receiving gain.

## 2.2 Dielectric Resonator Antenna (DRA)

Dielectric Resonator Antenna (DRA) is a radio antenna that consists of a block of ceramic material. It consists of various shapes such as hemispherical, cylindrical, and rectangular and so on. It is placed on a metal surface and it attached to a ground plane. Figure 2 below is the example of DRA fed with coaxial probe that attach to ground plane.



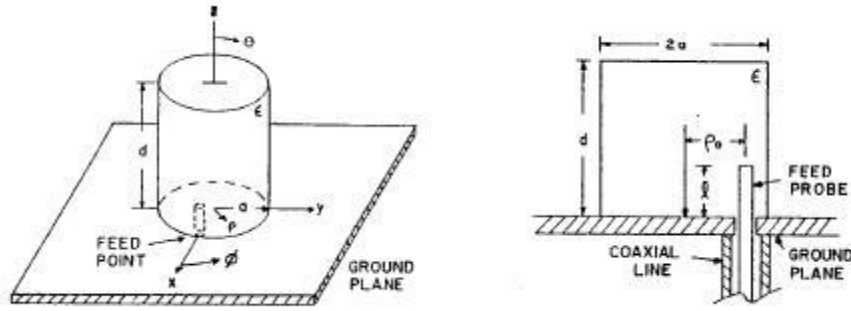


Figure 2 : DRA fed with coaxial probe and attach to ground plane

DRA is very useful for circuit applications, such as oscillators and filters, where it offers more compact alternative to the waveguide cavity resonator and it is more responsive technology for printed circuit integration [12][13][14]. Radio waves are passing through the resonator material from the transmitter circuit and then bounce back and forth between the resonator walls. From that it forms the standing waves. The resonator's walls are partially transparent to radio waves thus the radio power radiated into space [15].

There are several advantages of DRA. Below are the listed advantages of DRA:

- i. High degree of flexibility and versatility
  - Which allowing the designs to suit a wide range of physical or electrical requirements of varied communications applications.
- ii. Lack of metal parts
  - At high frequencies, the antenna will dissipate energy, or lossy.
  - At high microwave and millimeter frequencies, DRA will experiencing low losses and be more efficient than metal antenna.

### 2.3 Characteristics of DRA

DRA have several attractive characteristics. Below are the following characteristics of DRA:

- i. The DRA's size is directly proportional to  $\lambda_0/\sqrt{\epsilon_r}$ , where  $\lambda_0$  is the free-space wavelength at the resonant frequency, while  $\epsilon_r$  is the dielectric constant of the particular material.
- ii. For a fixed dielectric constant,  $\epsilon_r$ , the resonant frequency and the Q-factor will be affected by the aspect ratio of the DRA, later allow to add design flexibility.
- iii. Select a dielectric material with low-loss characteristics, high radiation efficiency can be obtained, even at millimeter-wave frequencies. It is due to an absence of surface waves and also minimum conductor losses contacted with the DRA.
- iv. Wide range of choice of dielectric constant .The value dielectric constant,  $\epsilon_r$  of DRA can be choose from 7 and above, which allow designers to control the size of the DRA and bandwidth.
- v. Can be operated in wide range of frequencies, from 1.3 GHz up to 40 GHz.
- vi. In order to excite the DRA, some of the feeding mechanism technique can be used for example slots, coplanar waveguide, microstrip, probes and dielectric image guides. This mechanism will improve the performance of the DRA and make them easily to integrate with various current technologies.
- vii. The DRA will radiate whether to short electric or magnetic dipoles if it chooses to excite by one specific mode. There are three modes that can excite within the DRA, it later will make the DRA produces whether directional or omnidirectional radiation patterns. It can be used to design for different coverage requirements.

## 2.4 Shapes of DRAs

There are three basic shapes of DRA which is hemispherical, cylindrical and rectangular. These are the basic shapes most commonly used.

### 2.4.1 Hemispherical Dielectric Resonator Antenna

In particular, the hemispherical DRAs have been studied, since exact analytical solutions only established to describe the several of field mode configurations, it used to predict the resonant frequency, radiation Q factor and radiation patterns of the DRA. For input impedance verification, probes and slot apertures can be used for various feed excitations. However, hemispherical provide limited practical value, it is because of the difficulty involved in fabrication and also lack of any degree freedom in choosing the design parameters. The radius of the sphere will determine the resonant frequency and radiation Q factor which will leave the designer have no control over the antenna size or the impedance bandwidth.

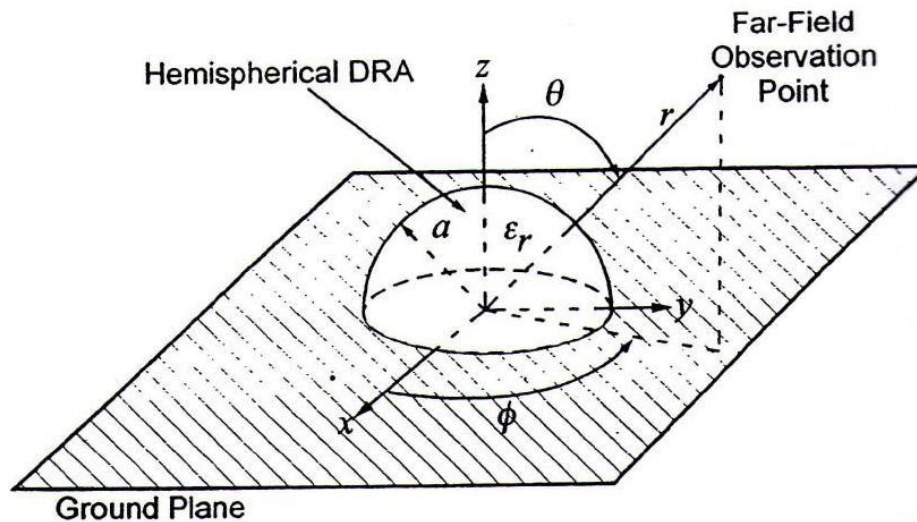


Figure 3 : Example of Hemispherical DRA shape

From Figure 3 above, the hemispherical DRA consists of a material with a dielectric constant of  $\epsilon_r$  and a radius of  $a$ . The hemispherical DRA is mounted on a ground plane.

### 2.4.1.1 Field Mode Configurations of Hemispherical DRA

In a dielectric sphere, the modes can be divided into two which are TE mode and TM mode. The TE modes are determined by having a zero value for radial component of the electrical field where  $E_r = 0$ , while the TM modes will have a zero radial component of the magnetic field where  $H_r = 0$ . The radiation pattern for TE is similar to a short horizontal magnetic dipole while the radiation pattern of TM modes is similar to a short electric monopole. Figure 4 below are the sketches of these patterns.

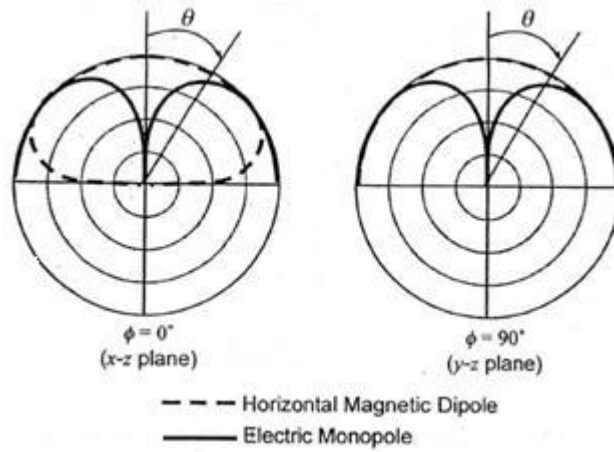


Figure 4 : Ideal radiation models of the dielectric resonator antenna on an infinite ground plane

#### 2.4.1.1.1 TE mode

The  $TE_{111}$  mode will produce a far field radiation pattern similar to that of a short horizontal magnetic dipole, and have a wide beam with a broadside peak. By solving the characteristic equation below, it will determine the resonant frequency and radiation Q factor for  $TE_{111}$  mode of hemispherical DRA.

$$\frac{J_{1/2}(\sqrt{\epsilon_r} k_0 a)}{J_{3/2}(\sqrt{\epsilon_r} k_0 a)} = \frac{H_{1/2}^{(2)}(k_0 a)}{\sqrt{\epsilon_r} H_{1/2}^{(2)}(k_0 a)} \quad (3)$$

Where:

$J(x)$  is the first-order Bessel function,

$H^{(2)}(x)$  is the second-order Hankel function,

$k_o a$  is the resonant frequency

$\epsilon_r$  is the dielectric constant

The resonant frequency  $f_{GHz}$  can be determined by using equation below:

$$f_{GHz} = \frac{4.7713 \text{Re}(k_o a)}{a_{cm}} \quad (4)$$

Then, the Q-factor  $Q$  can be found from equation below:

$$Q = \frac{\text{Re}(k_o a)}{2\text{Im}(k_o a)} \quad (5)$$

#### 2.4.1.1.2 TM mode

In  $TM_{101}$  mode of hemispherical of DRA will radiate like a short electric monopole antenna and is usually excite by place a probe located at the center of the DRA (at  $r=0$ ) [16]. For the  $TM_{101}$  mode case, the resonant frequency and radiation Q factor of the TM can be determined by solving a transcendental equation below:

$$\frac{1}{\sqrt{\epsilon_r} k_o a} - \frac{J_{1/2}(\sqrt{\epsilon_r} k_o a)}{J_{3/2}(\sqrt{\epsilon_r} k_o a)} = \frac{\sqrt{\epsilon_r}}{k_o a} - \sqrt{\epsilon_r} \frac{H_{1/2}^{(2)}(k_o a)}{H_{3/2}^{(2)}(k_o a)} \quad (6)$$

The resonant frequency and radiation Q-factor can be determined from equation below:

$$f_{GHz} = \frac{4.7713 \text{Re}(k_o a)}{a_{cm}} \quad (7)$$

$$Q = \frac{\text{Re}(k_o a)}{2\text{Im}(k_o a)} \quad (8)$$

## 2.4.2 Cylindrical Dielectric Resonator Antenna

The cylindrical dielectric resonator antenna provides greater design flexibility, where radius to height ratio controls the resonant frequency and the Q-factor. For a given resonant frequency and dielectric constant, different Q-factors can be acquired by varying the DRA's dimensions. Fabrication of cylindrical DRA is much simpler compared to hemispherical DRA. Various modes can be excited within the CDRA, later results in either omnidirectional or broadside radiation patterns.

It is described by a height  $h$ , a radius  $a$ , and a dielectric constant,  $\epsilon_r$ , as shown in Figure 5 below. This kind of shape provide one degree of freedom more than the hemispherical DRA where the aspect ratio  $a/h$  will determine the resonant frequency,  $k_0 a$  and the Q-factor for a known dielectric constant. Briefly, a tall and slender CDRA resonate the same frequency as a wide and thin CDRA. But these two cylindrical DRA will not have the same Q-factor.

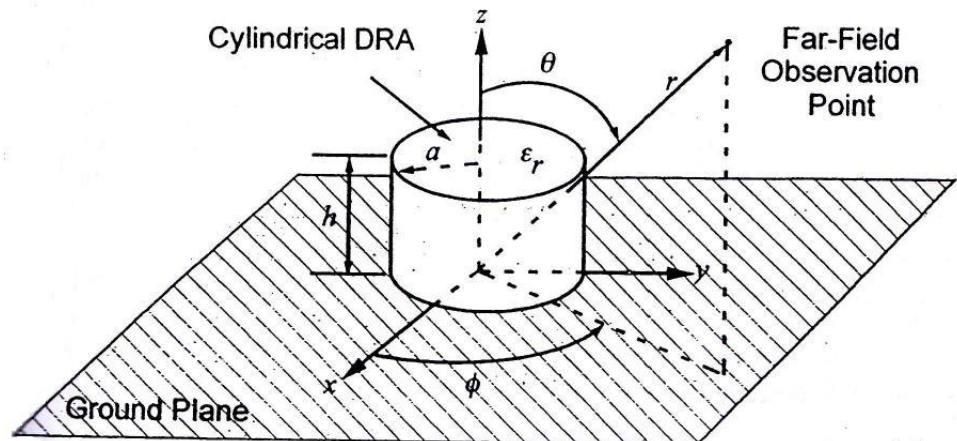


Figure 5 : Geometry of the cylindrical DRA

### 2.4.2.1 Field Mode Configurations of Cylindrical DRA

There are three types of modes of an isolated cylindrical DRA. They are TE mode, TM mode and HE mode [17]. The TE and TM modes are axially symmetric. Axially symmetric is no azimuthally dependence. Meanwhile the hybrid modes do have a dependence on azimuth. In hybrid modes, it refers to field variations in the

azimuth( $\theta$ ), radial ( $r$ ), and axial ( $z$ ) directions, respectively, in cylindrical coordinates.

#### 2.4.2.1.1 TE mode

In  $TE_{01\delta}$  mode, for cylindrical DRA, it will radiate similar to a short magnetic monopole. The equations for resonant frequency and Q-factor of this mode are taken from [17][18].

For resonant frequency:

$$k_o a = \frac{2.327}{\sqrt{\epsilon_r + 1}} \left\{ 1 + 0.2123 \frac{a}{h} - 0.00898 \left( \frac{a}{h} \right)^2 \right\} \quad (9)$$

While the Q-factor:

$$Q = 0.078192 \epsilon^{1.27} \left\{ 1 + 17.31 \left( \frac{h}{a} \right) - 21.57 \left( \frac{h}{a} \right)^2 + 10.86 \left( \frac{h}{a} \right)^3 - 1.98 \left( \frac{h}{a} \right)^4 \right\} \quad (10)$$

#### 2.4.2.1.2 TM mode

In  $TM_{01\delta}$  mode, for cylindrical DRA, it will radiate similar to a short electric monopole. The equations for resonant frequency and Q-factor are as follows (15):

Resonant frequency:

$$k_o a = \frac{\sqrt{3.83^2 + \left( \frac{\pi a}{2h} \right)^2}}{\sqrt{\epsilon_r + 2}} \quad (11)$$

Q-factor:

$$Q = 0.008721 \epsilon_r^{0.888413} e^{0.0397475 \epsilon_r} \left\{ 1 - \left( 0.3 - 0.2 \frac{a}{h} \right) \left( \frac{38 - \epsilon_r}{28} \right) \right\} \times \left( 9.498186 \frac{a}{h} + 2058.33 \left( \frac{a}{h} \right)^{4.32261} e^{-3.50099 \left( \frac{a}{h} \right)} \right) \quad (12)$$

### 2.4.2.1.3 HE mode

This project will be focusing on HE mode only. In  $HE_{11\delta}$  mode, a cylindrical DRA will produce a short horizontal magnetic dipole radiation that similar to the  $TE_{111}$  mode for hemispherical DRA [17]. The equation for resonant frequency and Q factor are as follows [17][18].

Resonant frequency:

$$k_o a = \frac{6.324}{\sqrt{\epsilon_r + 2}} \left\{ 0.27 + 0.36 \frac{a}{2h} + 0.02 \left( \frac{a}{2h} \right)^2 \right\} \quad (13)$$

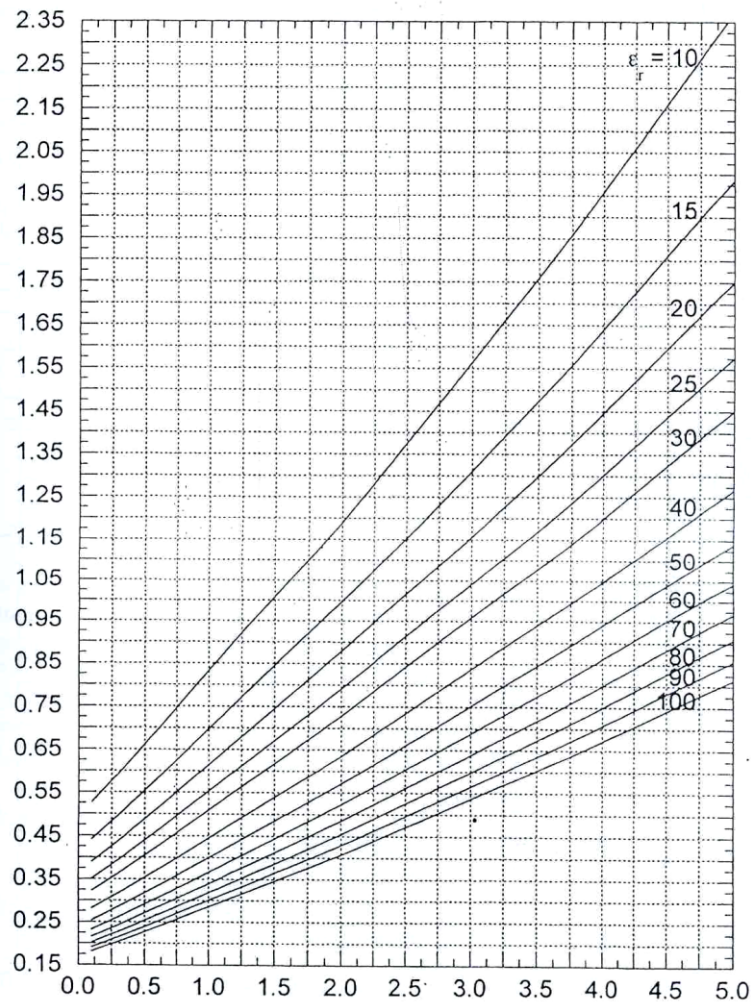


Figure 6 :  $k_o a$  of the  $HE_{11\delta}$  mode of the cylindrical DRA



Q-factor:

$$Q = 0.01007 \epsilon_r^{1.3} \frac{a}{h} \left\{ 1 + 100 e^{-2.05 \left( \frac{a}{2h} - \frac{1}{80} \left( \frac{a}{h} \right)^2 \right)} \right\} \quad (14)$$

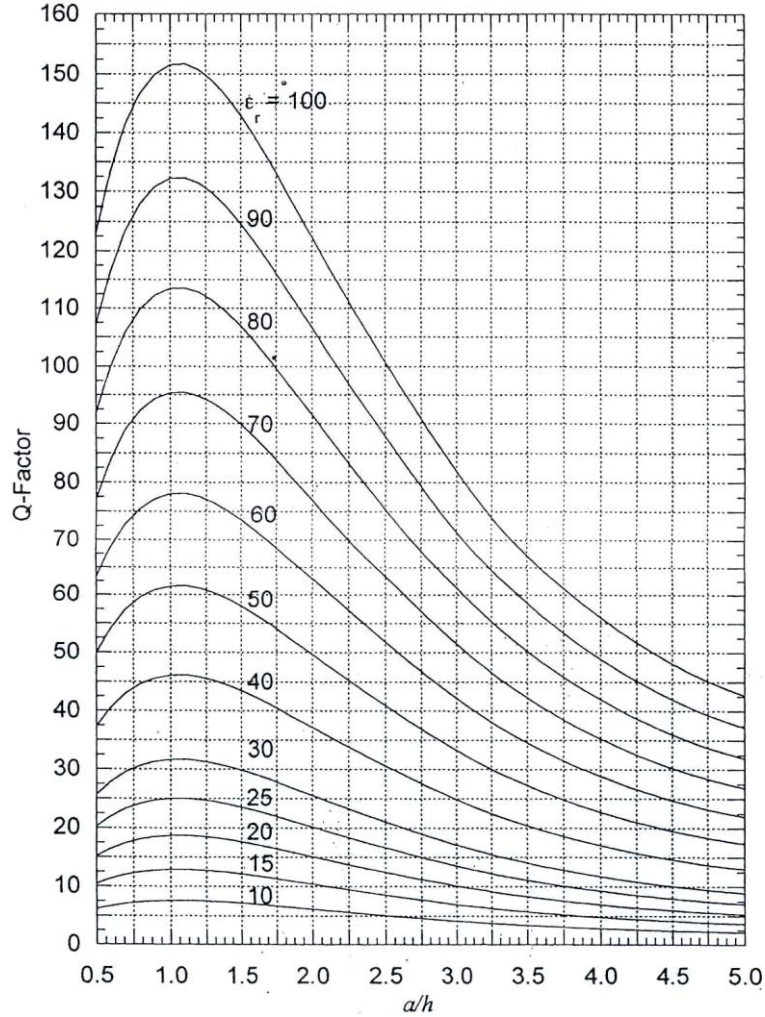


Figure 7 : Q-factor of the  $HE_{116}$  mode of the cylindrical DRA

### 2.4.3 Rectangular Dielectric Resonator Antenna

The rectangular dielectric resonator antenna (RDRA), bargains the greatest design flexibility of the three basic shapes. It has two degree of freedom which is length/width and depth/width. Several aspect ratios can be chosen to all resonate at a given frequency, while it offers different amount of radiation Q-factors for a given dielectric constant. Thus, this will leave designer with more options to create the desired DRA for particular application. It is described by a height  $h$ , a width  $w$ , a depth  $a$  and an electric constant  $\epsilon_r$ , as shown in Figure 8 below.

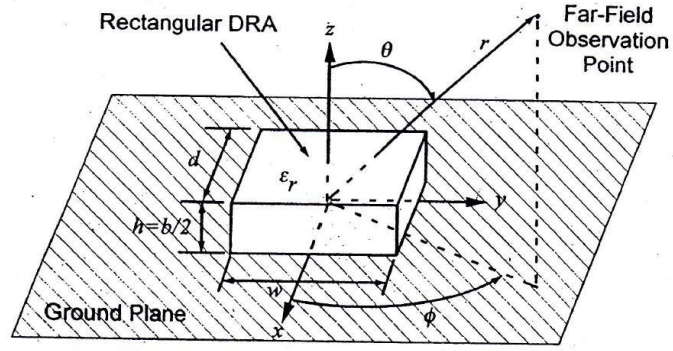


Figure 8 : Geometry for rectangular DRA

#### 2.4.3.1 Field Mode Configurations of Rectangular DRA

The rectangular DRA can be divided into TE and TM modes, but with the DRA mounted to the grounded plane, TE can only excite. The rectangular DRA can support  $TE^x$ ,  $TE^y$ , or  $TE^z$  modes. These modes then will radiate like a short magnetic dipole in the  $x$ -,  $y$ -, and  $z$ - directions respectively. The resonant frequency of each of these modes will later be a function of the DRA dimensions.

##### 2.4.3.1.1 TE mode

The resonant frequency,  $f_o$  for this mode can be obtained by solving the transcendental equation below:

$$k_x \tan(k_x d/2) = \sqrt{(\epsilon_r - 1)k_o^2 - k_x^2} \quad (15)$$

Where:

$$k_o = \frac{2\pi}{\lambda_o} = \frac{2\pi f_o}{c}$$

$$k_y = \frac{\pi}{w}$$

$$k_z = \frac{\pi}{b}$$

$$k_x^2 + k_y^2 + k_z^2 = \epsilon_r k_o^2$$

The normalized frequency,  $F$ , is defined as follow:

$$F = \frac{2\pi wf_o \sqrt{\epsilon_r}}{c} \quad (16)$$

After defined the normalized frequency,  $F$ , and then the Q-factor,  $f_{GHz}$  can determined by this equation:

$$f_{GHz} = \frac{15F}{w_{cm} \pi \sqrt{\epsilon_r}} \quad (17)$$

## 2.5 Coupling to DRAs

The coupling to DRAs will determined the radiation characteristics and the input impedance of the DRAs. It also has a significant impact on Q-factors and same goes to the resonant frequency. This will be done by selecting the proper feed mechanism and the determined the location of the feed on the circuit, which later plays important part to determine which mode will be excited.

### 2.5.1 Aperture Coupling

This is the common method to excite a DRA. The DRA will be excited through an aperture in the ground plane which the DRA is placed. Figure 9 below shows some of the aperture shaped that have been used for exciting DRAs. The small rectangular slot is the most widely used aperture so far [19]. By keeping the size of the slot electrically small, so the minimum amount of radiation going through below the ground plane occurred. Instead of rectangular slot, the annular slots have also been used widely for exciting DRAs [20], meanwhile cross-shaped and C-shaped slots are also used to excite the circular polarization [21]. The aperture slot shall be fed by a transmission line. It is either using microstrip or coaxial or a waveguide [22], as shown in Figure 9. This coupling mechanism provides the advantages of having the feed network located under the ground plane. It will isolate the radiating aperture from any unwelcome coupling or unwanted radiation from the feed. Figure 10, 11 and 12 are the examples of the aperture coupling to the other shapes of DRA.

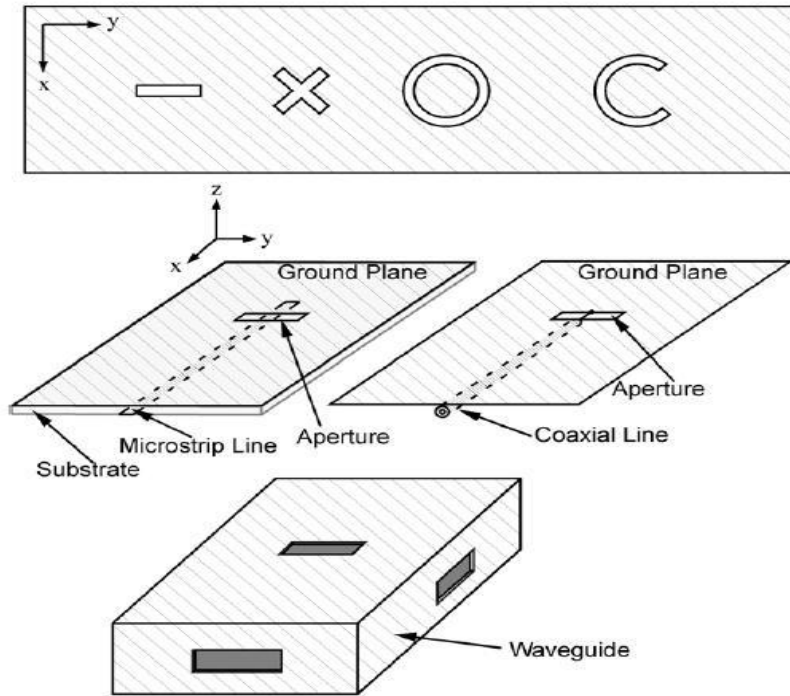


Figure 9 : Various slot apertures.

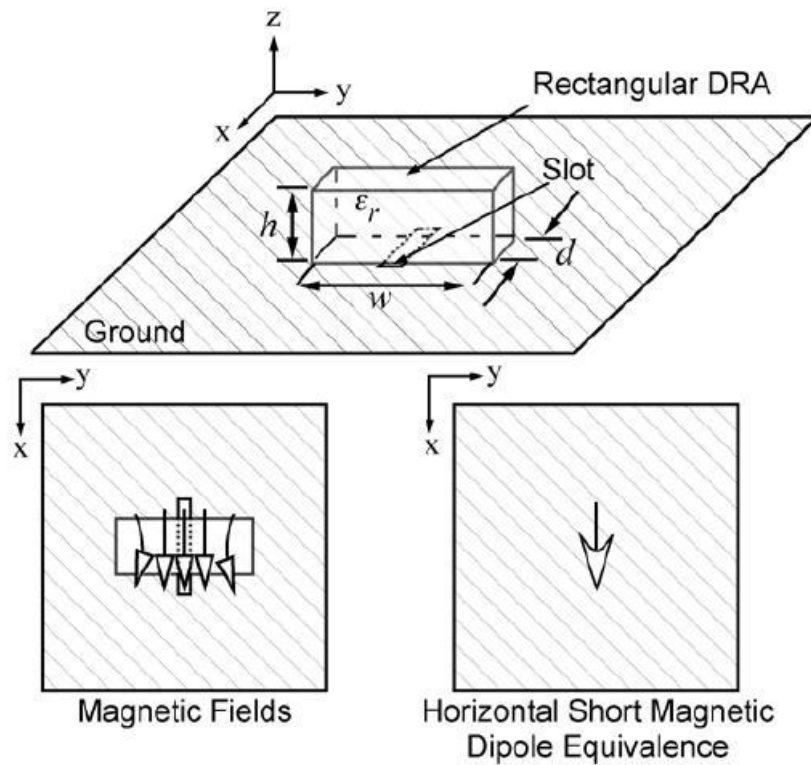


Figure 10 : Slot aperture coupling to a rectangular DRA

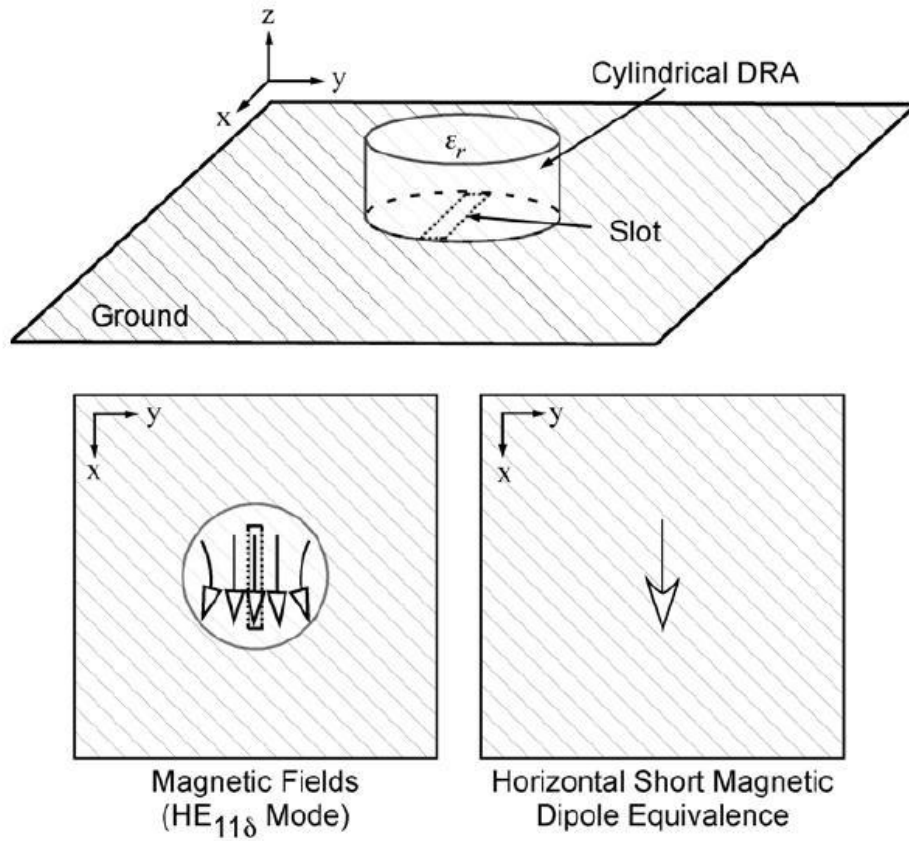


Figure 11 : Slot aperture coupling to a cylindrical DRA

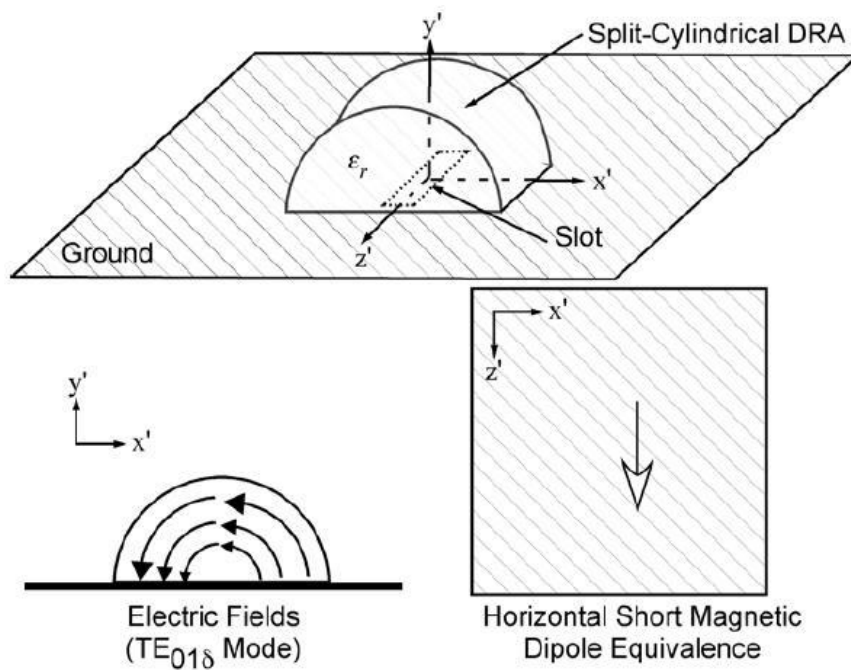


Figure 12 : Slot aperture coupling to a split-cylindrical DRA

## 2.5.2 Probe Coupling

Another method for coupling to DRAs is with a probe, as shown in Figure 13 [23]. The probe generally contains of the center pin of a coaxial transmission line that covers through the ground plane. The center pin can also be soldered together to a flat metallic strip that is placed nearby to the DRA [24]. In order to improve the impedance match, the length and the width shall be adjusted. The flat metal strip can also be connected to a microstrip line [25]. The probe can be considered as a vertical electric current, as the coupling purposes as shown in Figure 13. It must be located in a region of the DRA that experiencing high electric fields to obtain strong coupling. The probe can be located whether adjacent to the DRA or embedded within it. By adjusting the DRA location and the probe's height, the optimization of the coupling can be achieved. Apart from that, it also will depend on which modes can be excited and the location of the probe.

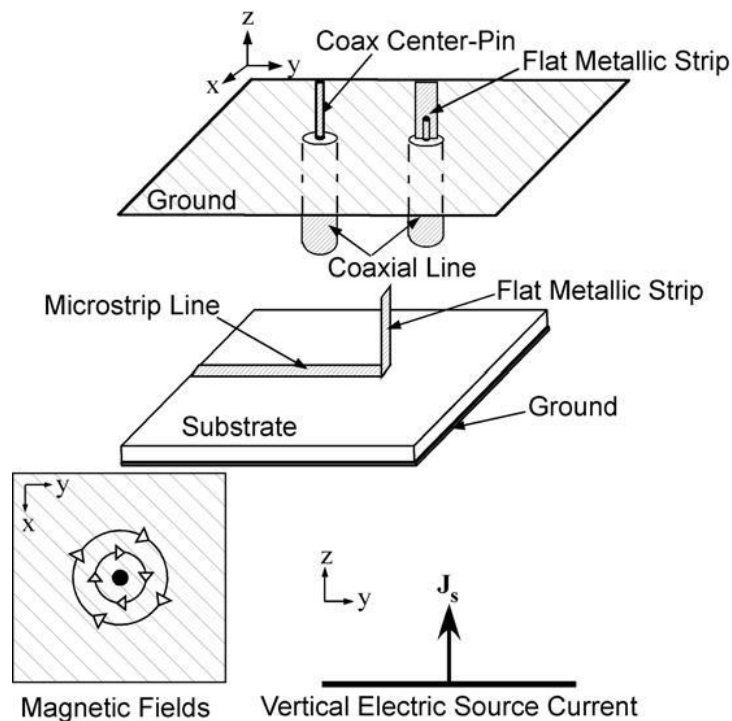


Figure 13 : Vertical probe sources

The length of probe is usually chosen to be less than the DRA's height. It is due to avoid any probe radiation. Analysis for probe-fed hemispherical and cylindrical DRAs have been done, the results show the effects of both the length and probe position on the resonant frequency and input impedance of the DRA [26]; but however there are still no simple calculations to design the required probe height for a

given set of DRA dielectric constant and its dimensions. Practically, placing the probe feed near to the DRA is preferable since it does not require any drilling into the DRA.

### 2.5.3 Microstrip Line Coupling

This is another common method for coupling to DRAs in microwave circuits. It is done by closeness coupling to microstrip lines. In Figure 14 shows the microstrip line coupling feeding technique that applied to DRAs [27]. This coupling technique can be used to excite the  $TE_{\delta 11}^x$  mode of the RDRA or the  $HE_{11\delta}$  mode of the CDRA, as shown in Figure 14. By adjusting  $s$  in the figure below, it can control the amount of the coupling from the microstrip line of the DRA. In figure below,  $s$  is representing spacing between the line and the DRA for the side coupled case. But for the direct coupled case,  $s$  is representing the length of the line underneath the DRA.

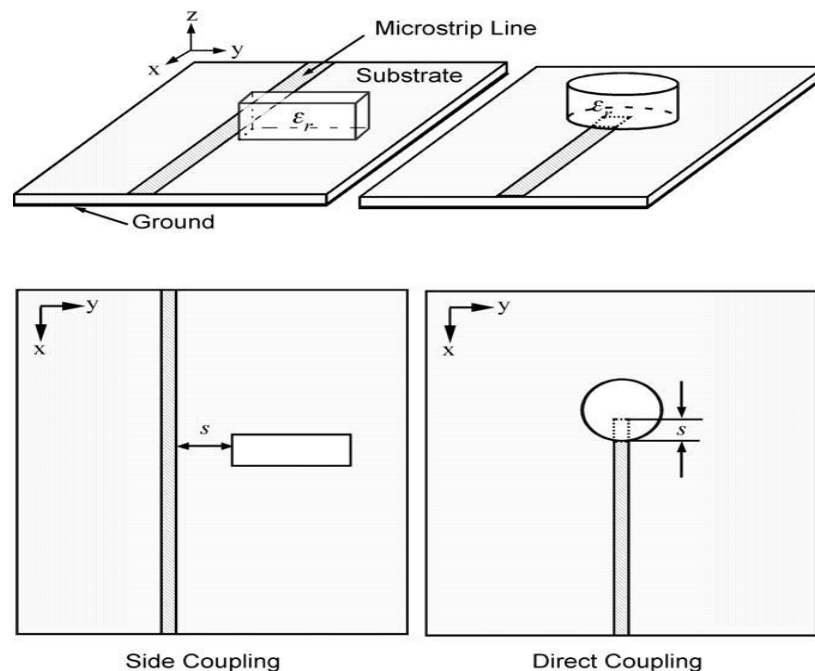


Figure 14 : Microstrip line coupling to DRAs

### 2.5.4 Coplanar Coupling

Coplanar coupling mechanism technique will be used in this project. Coupling to DRAs can also be accomplished by using coplanar feeds. Figure 15 below shows some of the examples of the coplanar coupling [28].

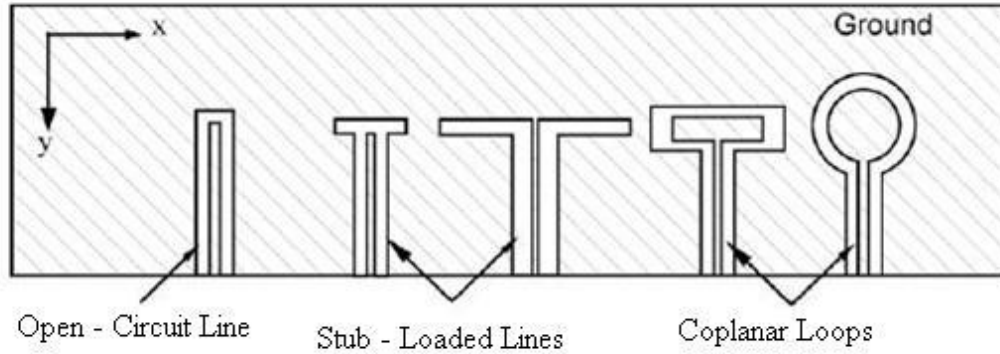


Figure 15 : Various coplanar feeds for coupling to DRAs

Open circuit coplanar waveguides can be used to directly feed the DRAs. By adding loops or stubs at the end of the line, the impedance matching can be controlled. In Figure 16 below, shows a CDRA being coupled to a coplanar loop. By adjusting the position of the DRA; the coupling level of the DRA can be controlled. The behavior of this coupling is similar to the coaxial probe. There is an advantage of the loop which it offers of being unobtrusive.

One can couple into either  $TE_{01\delta}$  or  $HE_{11\delta}$  mode of the cylindrical DRA by moving the loop from the edge of the DRA to the center [28]. The dimension of the coplanar feed must be chosen large enough to ensure proper coupling. And the dimension of the coplanar also can be chosen small enough to evade any excessive radiation in the back lobe. Refer Figure 16 below for coplanar loop coupling to a cylindrical DRA.

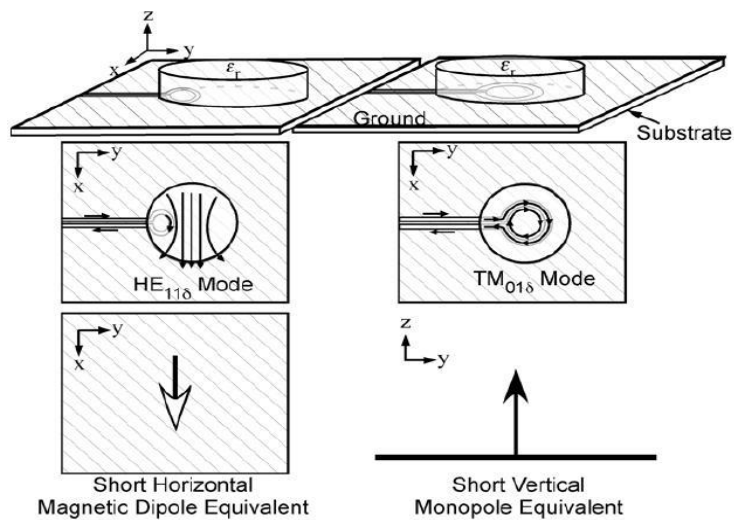


Figure 16 : Coplanar loop coupling to a cylindrical DRA



### 2.5.5 Dielectric Image Guide Coupling

Another way to couple to DRAs is by using a dielectric image guide, as presented in Figure 17. It offers advantages at millimeter-wave frequencies because they do not suffer from any conductor losses like microstrip coupling does. For microstrip lines, especially for the low dielectric constant DRAs, the amount of coupling to it is quite small. It would be possible to increase the coupling by operate the dielectric image guide closer to the cut off frequency. Thus, this coupling technique is the best choice to when make a linear array of DRAs.

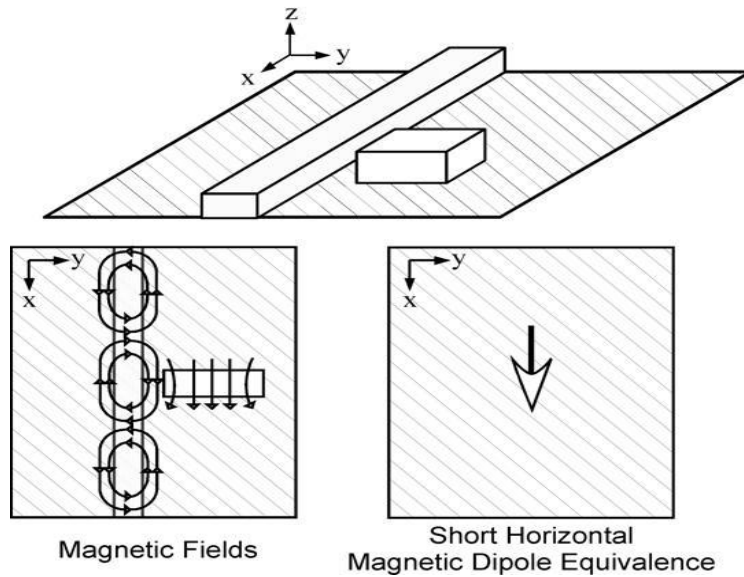


Figure 17 : Dielectric image guide feed for DRAs

## **CHAPTER 3**

### **METHODOLOGY**

#### 3.1 Research Methodology

In this project, the theoretical knowledge of the subject must be known and gained in order to get and know the idea of the project and also to achieve the main objective of this project. So, to grasp the theoretical knowledge of the subject, deep research and literature review has been done by reading all the writing material in the internet and library. For example, reading the related journal papers regarding designing and modeling of DRA, books of DRAs and anything related to this project in the web. The relevancy between selected papers, books and project objectives need to be taken into account to ensure the credibility of the project.

The Computer Simulation Technology (CST) Microwave Studio software also need to be studied since this software will be used to design and simulate the design of the CDRA later. In analysis stage, Agilent software will be used to obtain the equivalent circuit of the return loss of the simulation results. Microsoft Excel will be used to record all the results of return loss of the simulation. Later, the return loss's graph will be plotted by using the data. From the plotted graph, curve fitting method will be used to obtain the model. The curve fitting will generated the general equation of polynomial expression based on the graph plotted. Then, the parameters will be altered in order to make sure the model is valid. This method will analyze the result of the return loss to the field configuration mode which HE mode. After modeling of the CDRA is obtained, the parameters of the modeling will be tested back in order to verify the model. This is done by using the CST software.

### 3.2 Flow Chart

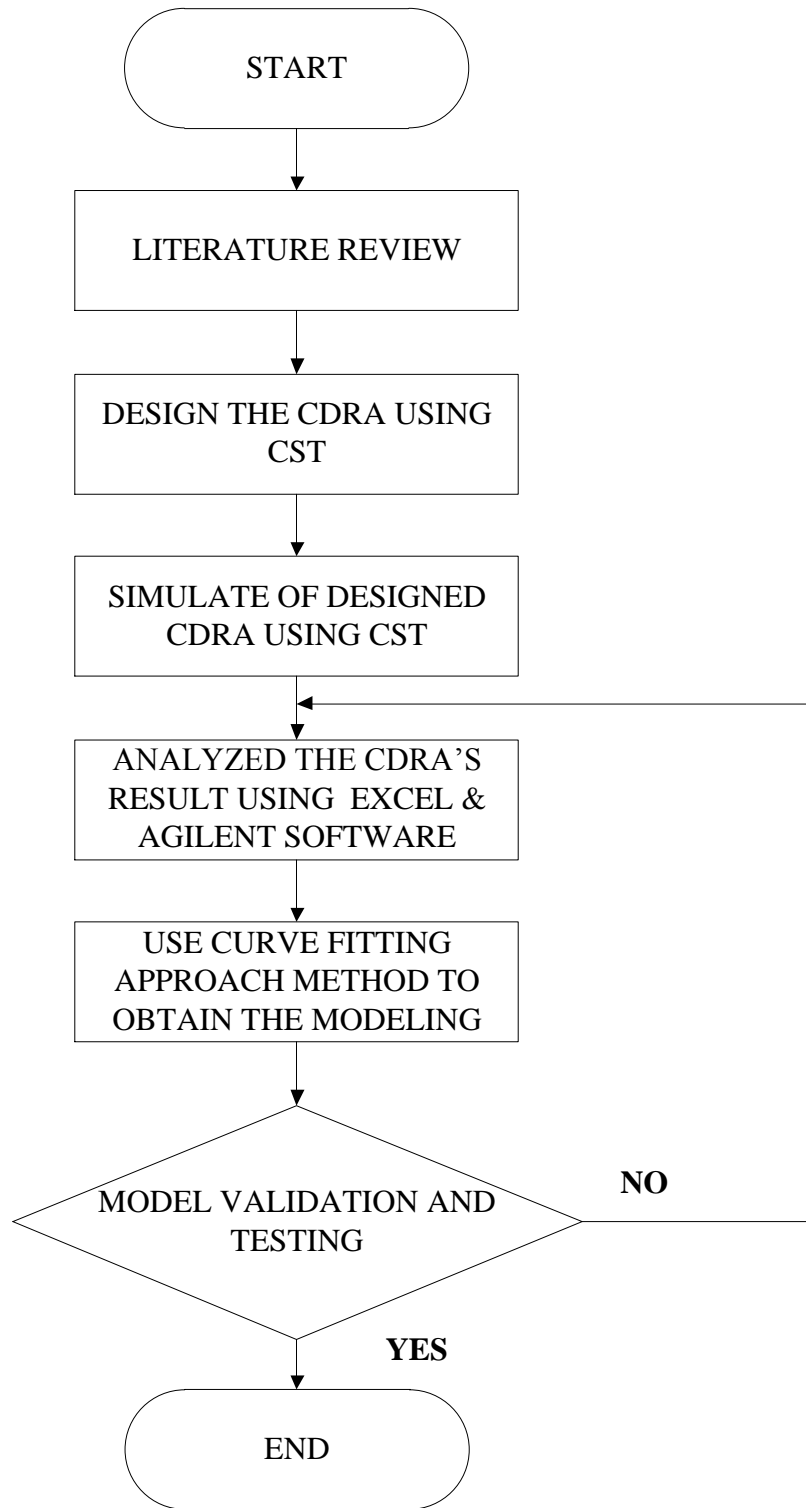


Figure 18 : Flow chart of designing and modeling a CDRA

### 3.2.1 Description of Flow Chart

Below is the brief explanation and description from the flow chart above:

#### 3.2.1.1 Literature review

Research and literature review is done to gain the understanding and knowledge of the project and also to determine the feasibility of the project. All the journals, books and web related to designing a CDRA and modeling were going through deeply in this stage.

#### 3.2.1.2 Design the CDRA using CST

In this step, the desired CDRA will be designed with specified resonant frequency and Q factor. The important parameter in designing CDRA is by choosing the suitable resonant frequency. In order to approximate the resonant frequency for the CDRA is by referring the equation 13. The expression of resonant frequency is calculated by:

$$f_r = \frac{6.324}{\sqrt{\epsilon_r + 2}} \left\{ 0.27 + 0.36 \frac{a}{2h} + 0.02 \left( \frac{a}{2h} \right)^2 \right\}$$

Where;

$f_r$  = resonant frequency

$\epsilon_r$  = resonator dielectric constant

a = radius of CDRA

h = height of CDRA

#### 3.2.1.2.1 CDRA with Microstrip Coupling Feed Technique

In this design, the dielectric material that been used is carbon base material. The carbon base CDRA is mounted on the ground plane. The ground plane is made from FR-4. Later, the CDRA excited by using a microstrip line. The parameters of the microstrip line coupling on the substrate are given as follows:

Resistive,  $R = 50 \Omega$ ;

Width,  $W = 11.9 \text{ mm}$

Thickness,  $h = 0.05$  mm

Length,  $l = 50$  mm start from bottom

Dielectric constant,  $\epsilon_{rs} = 3.8$

The CDRA is very efficient at millimeter wave frequencies, due to the reduction in metallic loss [29]. Initially, from the expression above, the resonant frequency that obtained from the calculation is 4.69 GHz. In order to make the CDRA operate at 2.45 GHz, a top metallic layer which is a layer of aluminum patch, is introduced at the top of the CDRA. This later will produce a lower resonant frequency and in advantage it allows the size of the CDRA to be reasonably in smaller dimension [30].

#### 3.2.1.2.2 CDRA with Coplanar Waveguide Coupling Technique

In this design, the dielectric material that been used is CCTO ( $\text{CaCu}_3\text{Ti}_4\text{O}_{12}$ ). The CCTO base CDRA is placed on the ground plane. The ground plane is made from FR-4. The CDRA later been excite by coplanar waveguide and also with microstrip feed line placed in between the CDRA and coplanar waveguide. The parameters of the CDRA with the microstrip line coupling on the substrate are given as follows:

Resistive,  $R = 50 \Omega$ ;

Width,  $W = 3.8$  mm

Thickness,  $h = 0.016$  mm

Length,  $l = 64.8$  mm start from bottom

Dielectric constant,  $\epsilon_{rs} = 3.8$

Same as the microstrip coupling feed technique, the CDRA is very efficient at millimeter wave frequencies, due to the reduction in metallic loss [29]. Initially, the calculated resonant frequency that obtained from the calculation is 4.89 GHz. In order to make the CDRA operate at 2.45 GHz, a top metallic layer which is a layer of aluminum patch, is introduced at the top of the CDRA. This later will produce a lower resonant frequency and in advantage it allows the size of the CDRA to be reasonably in smaller dimension [30].

### 3.2.1.3 Simulate the designed CDRA using CST

The designs of the CDRA above will be simulated by using CST Microwave Studio to obtain the result that later to be analyzed. The examples of results from the simulation are return loss, directivity, gain, smith chart, E – plane and H – plane. The obtained results later will be recorded for further discussion in Chapter 4.

### 3.2.1.4 Analyzed the CDRA's result using Microsoft Excel and Agilent software

In this stage, the data from return loss that obtained from the simulation being extracted. All the data been recorded in Microsoft Excel. Graph from the recorded data will be plotted.

The equivalent circuit will be obtained by using Agilent software. Before that, the data from the CST Microwave Studio will be exported to the Agilent software first in order to analyze the results.

### 3.2.1.5 Use curve fitting approach method to obtain the modeling

In this step, curve fitting method will be used to determine the model. There will be approximation of polynomial or exponential smoothing in order to obtain the model. The model will use the plotted graph of return loss to obtain the modeling.

### 3.2.1.6 Model validation and testing

After done with the modeling, the parameters from the modeling will be used to verify by using CST. In other word, the parameters from the modeling will be used to design a new CDRA by using CST software to verify the model.

### 3.3 Gantt chart and Milestone for Final Year Project I

#### 3.3.1 Gantt chart for Final Year Project I

Figure 19 below is the Gantt chart for Final Year Project I. Briefly; this is the timeline on every main activities and progress of completion of task that must be done according to the timeline given.

ACTIVITIES	FINAL YEAR PROJECT 1														
	WEEK NO.														
	1	2	3	4	5	6	7	8	9	10	11	12	13	14	
Literature Review and Background Study	→														
Design the CDRA using Computer Simulation Technology (CST) software						→									
Simulation of the DRA using Computer Simulation Technology (CST) Software								→							
Report Writing								→							

Figure 19 : Gantt chart for Final Year Project I

### 3.3.2 Milestone for Final Year Project I

Below is the Milestone for Final Year Project I. Milestone indicating the entire task's due time. So, the entire task must be completed before the due date.

Table 1 : Milestone for Final Year Project I

<b>Component Submission</b>	<b>Time (Week)</b>
Completion of Literature Review and Background Study	Week#7
Completion of Design of the DRA using Computer Simulation Technology (CST) software	Week #10
Completion of Simulation of the DRA using Computer Simulation Technology (CST) software	Week#14
Documentation	Week#14



### 3.4 Gantt chart for Final Year Project II

#### 3.4.1 Gantt chart

Figure 20 below is the Gantt chart for Final Year Project II.

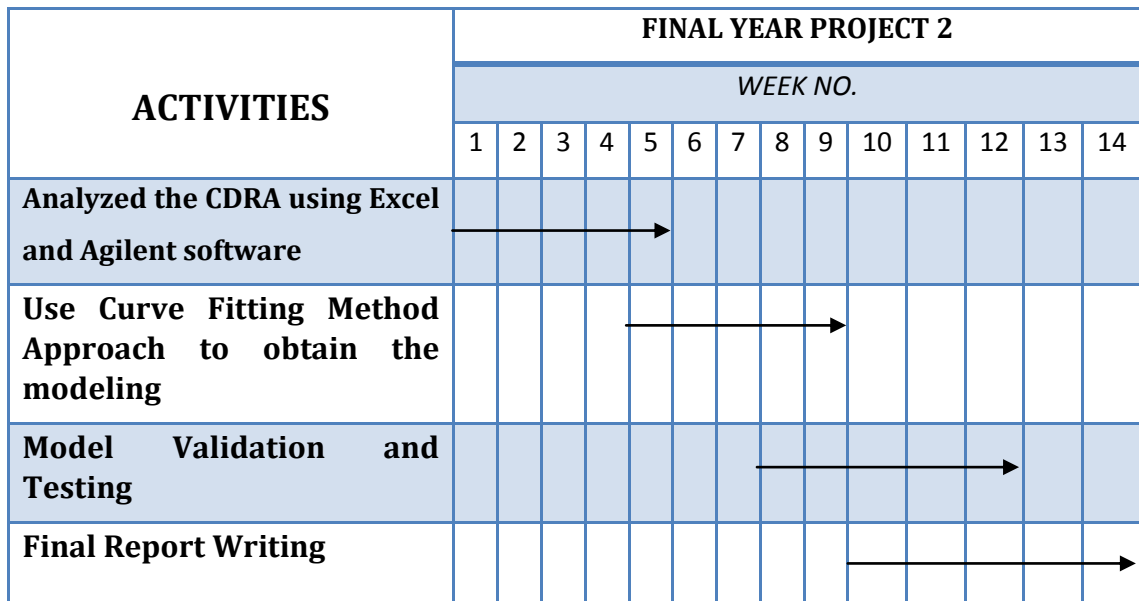


Figure 20 : Gantt chart for Final Year Project II

#### 3.4.2 Milestone for Final Year Project II

Below is the Milestone for Final Year Project II.

Table 2 : Milestone for Final Year Project II

Component Submission	Time (Week)
Completion of Analyzed the DRA using MATLAB/ Excel/ Agilent	Week#5
Completion of modeling by using Curve Fitting Method Approach	Week #9
Completion of Model Verification and Testing	Week#12
Documentation	Week#14

### 3.5 Tools

The main software in order to accomplish this project is Computer Simulation Technology (CST) Microwave Studio software. This software will be used at the early stage and the end of the project. This software will help to design and simulate the desired CDRA. Besides, Microsoft Excel will be used in the analysis stage. Agilent software also can be used instead of using Microsoft Excel. The other tool needed is a personal computer.

### 3.6 Project Schedule

The planned schedule for Final Year Project I and II are as follows:

Table 3 : Project schedule for Final Year Project I

<b>Component Submission</b>	<b>Time (Week)</b>
Title Selection	Week 1
Extended Proposal	Week 6
Proposal Defense	Week 9
Draft Report	Week 13
Final Report	Week 14

Table 4 : Project schedule for Final Year Project II

<b>Component Submission</b>	<b>Time (Week)</b>
Pre-EDX	Week 8
Draft Report	Week 13
Final Report	Week 14
VIVA	Week 15

## **CHAPTER 4**

### **RESULT AND DISCUSSIONS**

#### 4.1 Cylindrical Dielectric Resonator Antenna with Microstrip Coupling

##### 4.1.1 Antenna Structure

Figure 21 below showed the cylindrical dielectric resonator antenna with microstrip feeding technique designed by using CST software. The material for the dielectric resonator antenna (DRA) is carbon with  $\epsilon = 7.0$  (dielectric constant). The radius of the DRA is 14.125 mm. Meanwhile the thickness of the DRA is 2.5 mm. A layer of aluminum is patched on top the DRA and the thickness of the aluminum is 0.1 mm. The feeder is made from copper while the ground plane is made from lossy metal. The purpose of selecting copper and lossy metal as material because they have the ability to minimize power dissipation, improve reliability, good conductor and affordable.

The width and length of the ground plane is designed to have 50 mm and 60 mm respectively with its thickness is 1 mm. The ground plane uses of Rogers RO4003 (lossy) as material at the front surface while at the back the material used is copper. Rogers RO4003 (lossy) dielectric constant is approximately equal to 1 at 2.45 GHz frequency which means the dielectric tolerance and loss can be ignored [31]. The feeder width and length is designed to be 11.9 mm and 50 mm respectively while the DRA is position approximately at 32 mm from bottom.

The rectangular and circle slots are made at the back of the antenna with the rectangular slot dimension is 4 mm width and 13 mm length while the circle slot dimension is 4.5 mm radius. The rectangular slot is position 21mm from top and the circle is placed at 22 mm from bottom of the ground plane. Please refer to Figure 22 for further understanding.

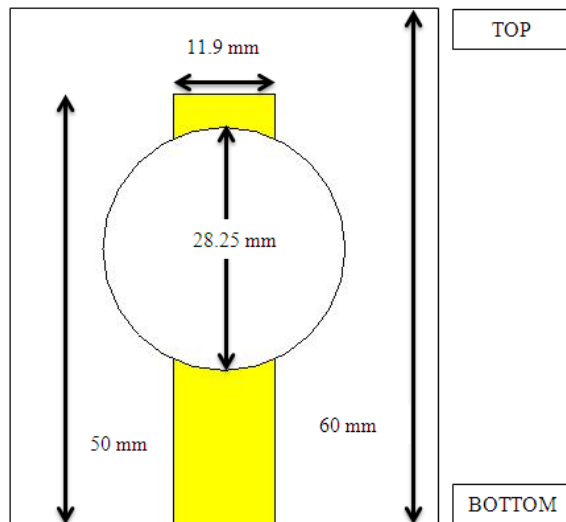


Figure 21 : Front view of CDRA with microstrip coupling designed using CST

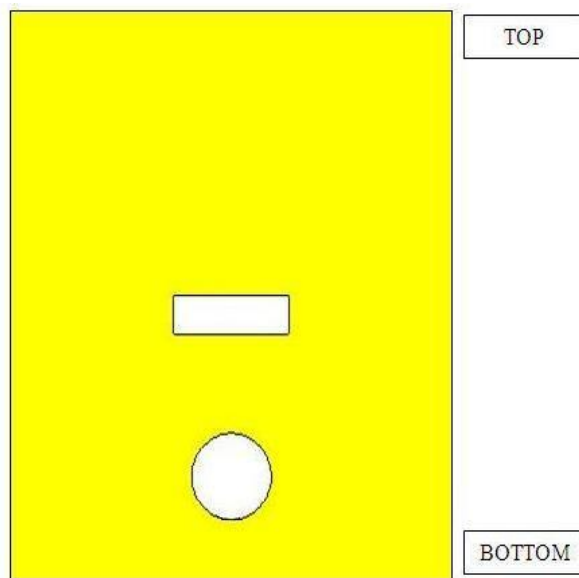


Figure 22 : Back view of CDRA with microstrip coupling designed using CST

Later the results that will be discussed are the return loss and farfield. Explanation below will elaborate more on these two concepts.

a) Return Loss

Return loss is the measurement of the ability of the receiving end to absorb the transmitted signal. Some of the signal will be reflected back where this signal will

create interference either constructive interference or destructive interference that can produce error in measurement. It is important to measure the return loss in order to determine the exact value of signal received at the receiver end. The S-parameter (scatter matrix) will be used to calculate the magnitude of the loss signal where the x-axis shows the frequency when the highest magnitude of the loss signal occurred.

b) Farfield

Farfield is the region where the signal radiation creates uniform pattern. The farfield indicates where the signal will dissipate before the signal totally disappears to the open space. The maximum farfield frequency simulation result is at 2.45 GHz. The red color indicates the strongest signal simulated while the blue signal indicates the weakest signal produced. The DRA is directional, thus the front side which is in the same direction of the antenna directivity has the strongest signal while the back of the DRA has weaker signal as the direction is opposite to the DRA directivity. Refer to Figure 22 below for the color indication for signal strength.

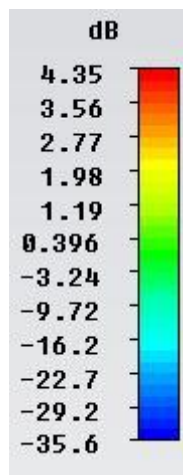


Figure 23 : The signal indication for signal strength (refer to the color only)

#### 4.1.1.1 Result of the CDRA with microstrip coupling

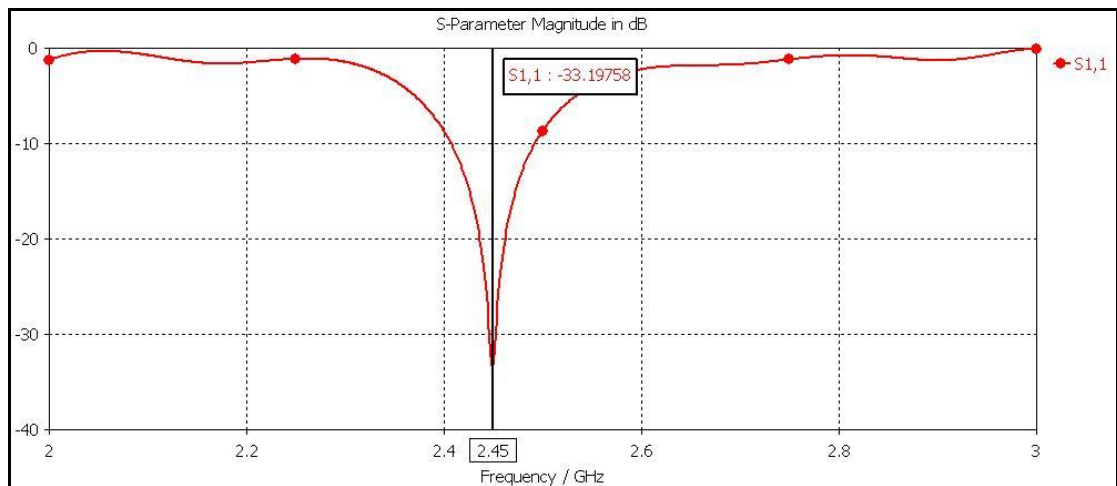


Figure 24 : Return Loss of the CDRA with microstrip coupling

Figure 24 above show the result of return loss of the CDRA with microstrip coupling that obtained from CST simulation. After obtained the return loss's result of the CDRA with microstrip coupling, all the data have been taken to be recorded. Refer Table 10 for the recorded data. A plotted graph has been obtained by using all the recorded data from Table 10 by using Microsoft Excel. Please refer Figure 38 to see the plotted graph.

The simulated return loss of the DRA is obtained in Figure 24. This antenna achieves a -33.1976 dB return loss at resonant frequency 2.45 GHz. The simulated value is acceptable since it is lower than -10dB. -10 dB is the reference value for an antenna to starts transmits the signal. The gain simulated for the CDRA is 5.335 dB at resonant frequency 2.45GHz. Refer Figure 25 for further information about the result of the gain. The radiation efficiency for the CDRA is -0.9284 dB while the total efficiency of the DRA is -0.934 dB. Figure 26 show the directivity of the CDRA is 6.263 dBi. The directivity value must be above 5 dBi in order to make it good antenna.

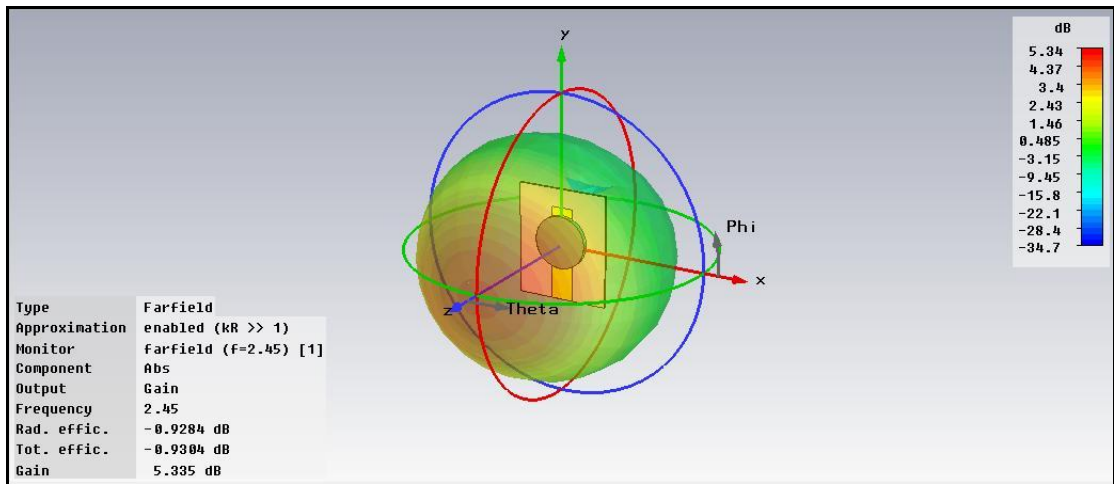


Figure 25 : Gain of the CDRA with microstrip coupling

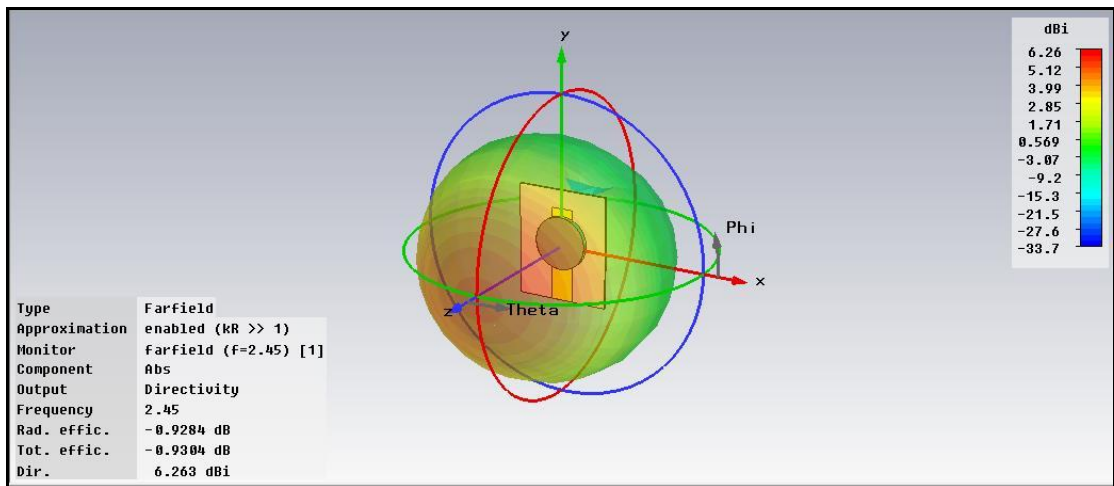


Figure 26 : Directivity of the CDRA with microstrip coupling

There is also a relationship between the resonant frequencies and the position of the rectangular slot and also the size of the rectangular slot in term of return loss. In this case, the position of the DRA is not moving. Initially, the position of the rectangular slot is at 35 mm above the ground plane. During this process, the size of the rectangular slot has been increased by +1 mm horizontally. Originally, the rectangular slot size is 13 mm x 4 mm. Then the size of the rectangular slot is increased by +1 mm by length, up to 17 mm x 4 mm. After the whole simulation at this phase finished, the slot will be move down -1 mm vertically until the position of the DRA at 31 mm from the bottom of the ground plane. Refer figures below for further information.

Figure 27, showed the indications to help understand the Figure 28, 30, 32, 34 and 36. It indicates about the size of slot expansion horizontally.

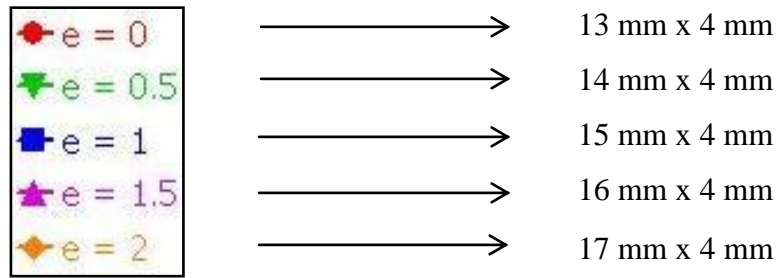


Figure 27 : Legends that refers to the size of slot expansion

Refer Figure 28 below for result of return loss of the expansion of rectangular slot when its position is at 39 mm from top. From Figure 28, it can be concluded that as, the bigger the slot size, the lower the resonant frequency.

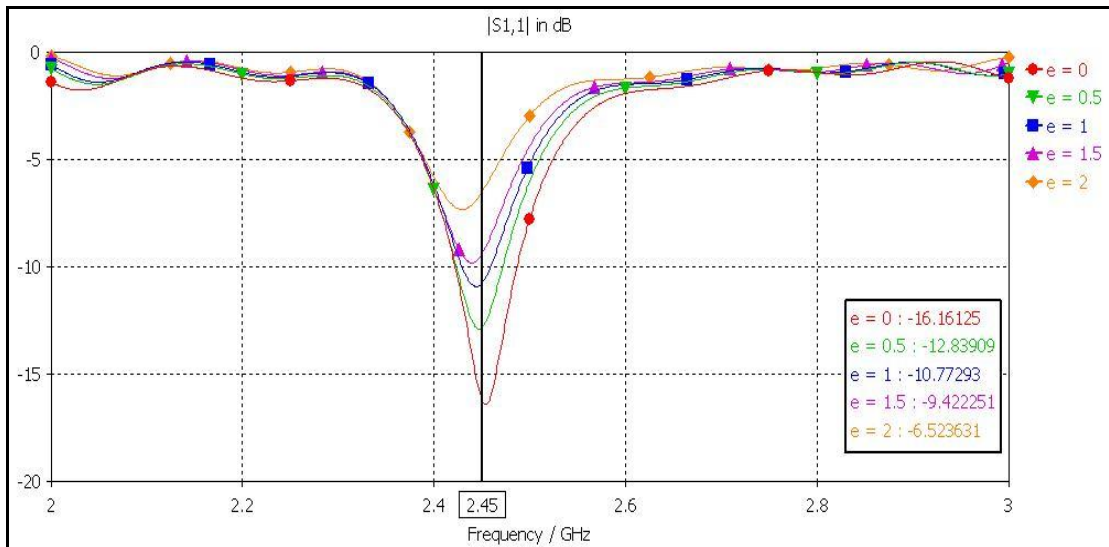


Figure 28 : Return loss when the slot at 39 mm from top

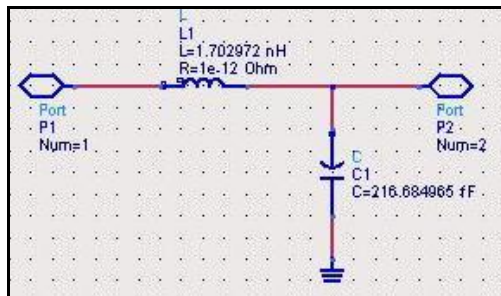


Figure 29 : The equivalent circuit when slot at 39 mm from top

In Table 5 showed that the values of return loss of the expansion of rectangular slot at 2.45 GHz. Based on the observation from Table 5, the smaller the rectangular slot size, the lower the return loss value.



Table 5 : Results of Simulated Return Loss at 2.45 GHz

Rectangular Slot Position	Rectangular Slot Size	Simulated Return Loss at 2.45 GHz
39 mm from top	13 mm x 4 mm	-16.16125 dB
	14 mm x 4 mm	-12.83909 dB
	15 mm x 4 mm	-10.77293 dB
	16 mm x 4 mm	-9.422251 dB
	17 mm x 4 mm	-6.523631 dB

As Figure 28, refer Figure 30 below for result of return loss of the expansion of rectangular slot when its position is at 40 mm from top. From Figure 30, it can be concluded that as, the bigger the slot size, the lower the resonant frequency.

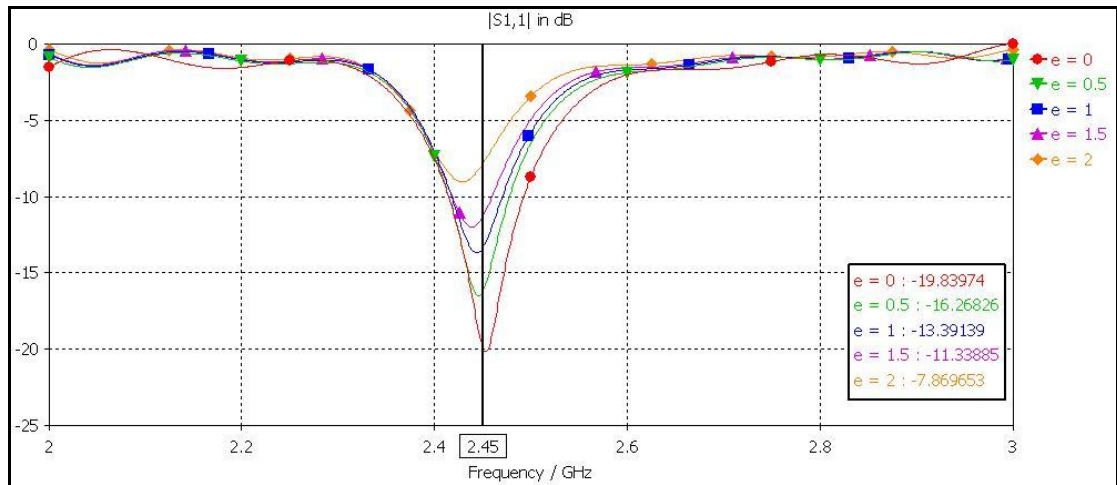


Figure 30 : Return loss when the slot at 40 mm from top

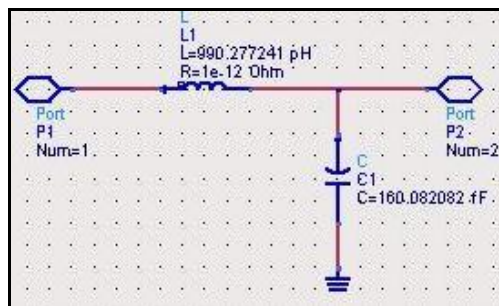


Figure 31 : The equivalent circuit when slot at 40 mm from top

In Table 6 showed that the values of return loss of the expansion of rectangular slot at 2.45 GHz. Based on the observation from Table 6, the smaller the rectangular slot

size, the lower the return loss value.

Table 6 : Results of Simulated Return Loss at 2.45 GHz

Rectangular Slot Position	Rectangular Slot Size	Simulated Return Loss at 2.45 GHz
40 mm from top	13 mm x 4 mm	-19.83974 dB
	14 mm x 4 mm	-16.26826 dB
	15 mm x 4 mm	-13.39139 dB
	16 mm x 4 mm	-11.33885 dB
	17 mm x 4 mm	-7.869653 dB

Refer Figure 32 below for result of return loss of the expansion of rectangular slot when its position is at 41 mm from top. From Figure 32, it can be concluded that as, the bigger the slot size, the lower the resonant frequency.

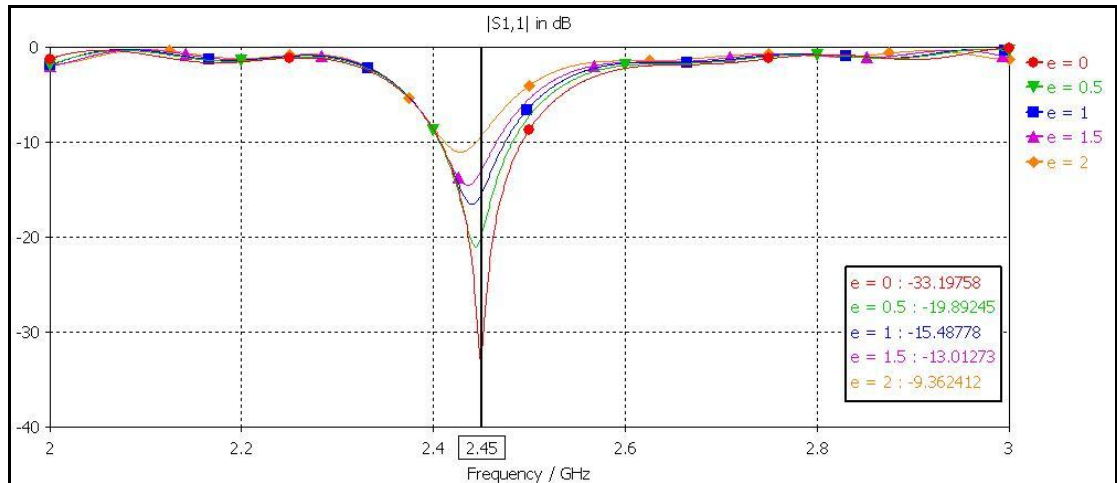


Figure 32 : Return loss when the slot at 41 mm from top

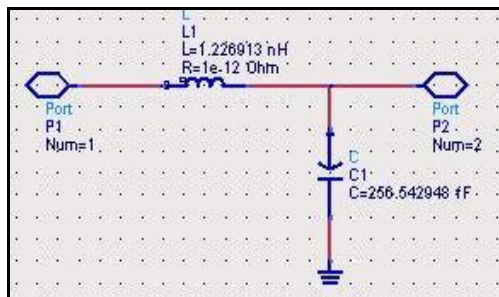


Figure 33 : The equivalent circuit when slot at 41 mm from top

In Table 7 showed that the values of return loss of the expansion of rectangular slot at 2.45 GHz. Based on the observation from Table 7, the smaller the rectangular slot size, the lower the return loss value.

Table 7 : Results of Simulated Return Loss at 2.45 GHz

Rectangular Slot Position	Rectangular Slot Size	Simulated Return Loss at 2.45 GHz
41 mm from top	13 mm x 4 mm	-33.19758 dB
	14 mm x 4 mm	-19.89245 dB
	15 mm x 4 mm	-15.48778 dB
	16 mm x 4 mm	-13.01273 dB
	17 mm x 4 mm	-9.362412 dB

Refer Figure 34 below for result of return loss of the expansion of rectangular slot when its position is at 42 mm from top. From Figure 34, it can be concluded that as, the bigger the slot size, the lower the resonant frequency.

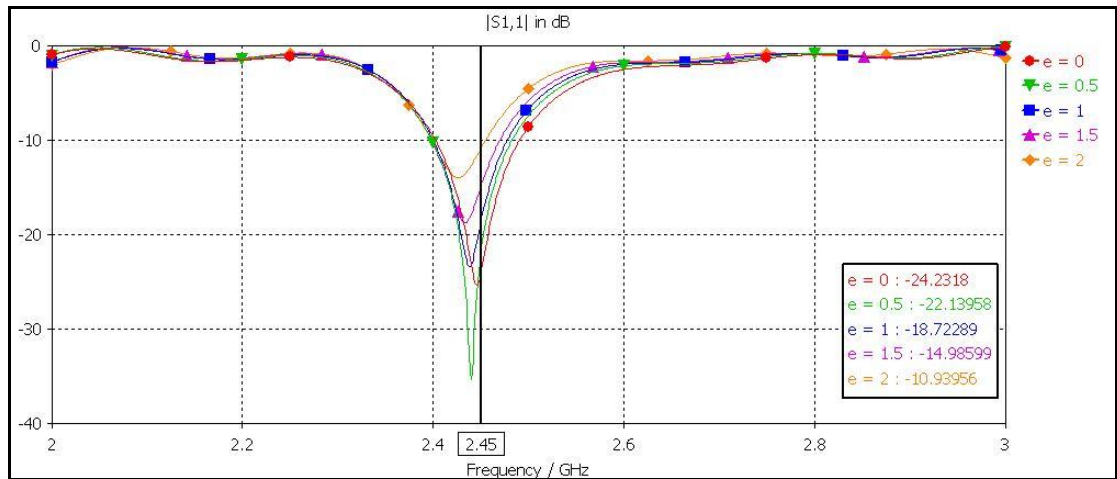


Figure 34 : Return loss when the slot at 42 mm from top

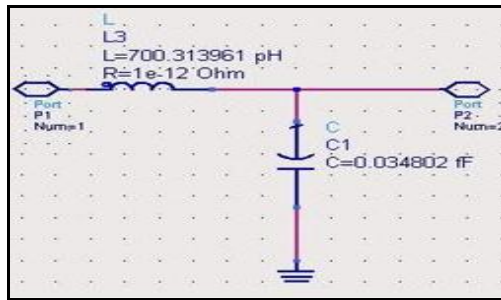


Figure 35 : The equivalent circuit when slot at 42 mm from top

In Table 8, showed that the values of return loss of the expansion of rectangular slot at 2.45 GHz. Based on the observation from Table 8, the smaller the rectangular slot size, the lower the return loss value.

Table 8 : Results of Simulated Return Loss at 2.45 GHz

Rectangular Slot Position	Rectangular Slot Size	Simulated Return Loss at 2.45 GHz
42 mm from top	13 mm x 4 mm	-24.2318 dB
	14 mm x 4 mm	-22.13958 dB
	15 mm x 4 mm	-18.72289 dB
	16 mm x 4 mm	-14.98599 dB
	17 mm x 4 mm	-10.93956 dB

Refer Figure 36 below for result of return loss of the expansion of rectangular slot when its position is at 43 mm from top. From Figure 36, it can be concluded that as, the bigger the slot size, the lower the resonant frequency.

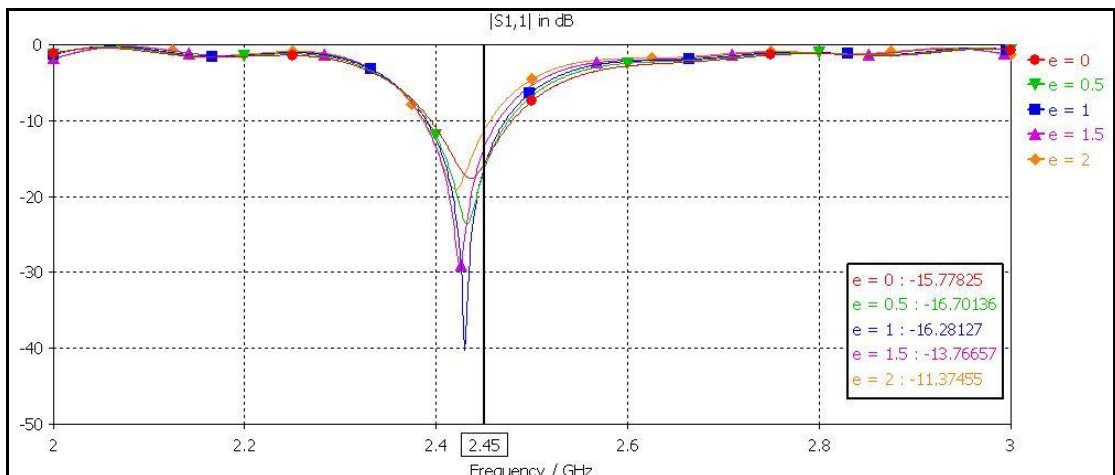


Figure 36 : Return loss when the slot at 43 mm from top

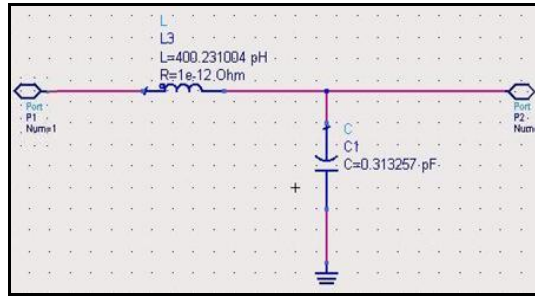


Figure 37 : The equivalent circuit when slot at 43 mm from top

In Table 9, showed that the values of return loss of the expansion of rectangular slot at 2.45 GHz. Based on the observation from Table 9, the smaller the rectangular slot size, the lower the return loss value.

Table 9 : Results of Simulated Return Loss at 2.45 GHz

Rectangular Slot Position	Rectangular Slot Size	Simulated Return Loss at 2.45 GHz
43 mm from top	13 mm x 4 mm	-15.778325 dB
	14 mm x 4 mm	-16.70136 dB
	15 mm x 4 mm	-16.28127 dB
	16 mm x 4 mm	-13.76657 dB
	17 mm x 4 mm	-11.37455 dB

Based from Figure 28 – 37 and Table 5 – 9 above, showed the results of the return loss and the equivalent circuit of each phase. The equivalent circuit of the rectangular slot is constructed referring to the results of return loss obtained. All the equivalent circuit above will be connected to the 50  $\Omega$  resistor in parallel. The circuit represents the frequency tuning capability of the slot and it has its own impedance matching. If the value of the capacitance,  $C$  is adjusted, it will affect the return loss. And if the value of the inductance,  $L$  is adjusted, it will affect the value of the resonant frequency.

There are two separate observations, which are in term of resonant frequency and return loss. In term of resonant frequency, in order to make it fall into 2.45GHz, the lower the position of the slot from bottom, the higher the resonant frequency will be

diverted, thus slot size must be bigger. In term of return loss, the lower the position of the slot from bottom, the lesser value of the return loss in dB.

Table 10 : Recorded data from the return loss of the CDRA

Resonant Frequency GHz	S <sub>1,1</sub> dB
2.2	-1.5576
2.21	-1.4738
2.22	-1.3813
2.23	-1.291
2.24	-1.2132
2.25	-1.1576
2.26	-1.1326
2.27	-1.1458
2.28	-1.2039
2.29	-1.3134
2.3	-1.4806
2.31	-1.7116
2.32	-2.0136
2.33	-2.3945
2.34	-2.864
2.35	-3.4339
2.36	-4.1198
2.37	-4.9428
2.38	-5.932
2.39	-7.1304
2.4	-8.6044
2.41	-10.4655
2.42	-12.9222
2.43	-16.4387
2.44	-22.4251
2.45	-33.1976

2.46	-21.5883
2.47	-16.0887
2.48	-12.7899
2.49	-10.4749
2.5	-8.7239
2.51	-7.3438
2.52	-6.2293
2.53	-5.3174
2.54	-4.5664
2.55	-3.9477
2.56	-3.4402
2.57	-3.0277
2.58	-2.6975
2.59	-2.4386
2.6	-2.2412
2.61	-2.0963
2.62	-1.9953
2.63	-1.9294
2.64	-1.8897
2.65	-1.8672
2.66	-1.853
2.67	-1.8387
2.68	-1.8168
2.69	-1.7813
2.7	-1.7283

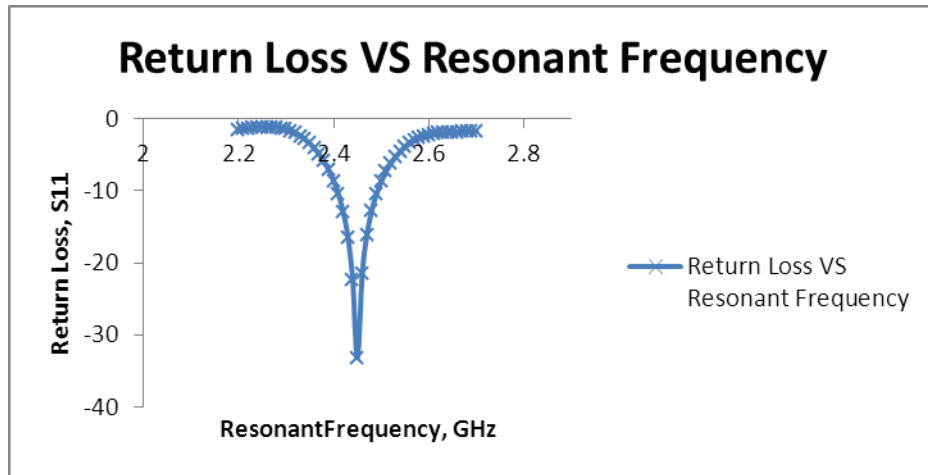


Figure 38 : Plotted graph of CDRA by using Microsoft Excel

From the plotted graphs above, the mathematical equation can be obtained. Thus, the mathematical modeling equation of CDRA using microstrip coupling has been obtained by using curve fitting method. The general equation of polynomial expression has been generated by using Microsoft Excel based on the plotted graph. The 6<sup>th</sup> order polynomial equation appears as result of modeling. By altering the parameter's constant of the 6<sup>th</sup> order polynomial expression to get the model as close as possible to the original simulated return loss result. Below is the mathematical modeling equation of CDRA using microstrip coupling.

$$y = 442111x^6 - 6e^6x^5 + 3.97e^7x^4 - 1.3e^8x^3 + 2.37e^8x^2 - 2.31e^8x + 9e^7 \quad (18)$$

Where;

$$P_1 = 442111$$

$$P_2 = -6e^6$$

$$P_3 = 3.97e^7$$

$$P_4 = -1.3e^8$$

$$P_5 = 2.37e^8$$

$$P_6 = -2.31e^8$$

$$P_7 = 9e^7$$



In model above,  $y$  represents return loss of the CDRA while  $x$  represents the resonant frequency.

Table 11 : Analysis of modeling for Microstrip

Polynomial Order	Model	Accuracy Result, %
1 <sup>st</sup> order	$y = -1.67 - 1.57x$	10%
2 <sup>nd</sup> order	$y = 1.23e^3 - e^3x + 2.05e^2x^2$	23%
3 <sup>rd</sup> order	$y = 6e^2 - 3.1e^2x + 8ex^2 - 3.88ex^3$	35%
4 <sup>th</sup> order	$y = -3.53e^5 + 5.85e^5x - 3.57e^5x^2 + 9.7e^4x^3 - 10e^3x^4$	60%
5 <sup>th</sup> order	$y = -4.67e^5 + 8.17e^5x - 5.5e^5x^2 + 1.7e^5x^3 - 2.6e^4x^4 + 1.32e^3x^5$	83%
6 <sup>th</sup> order	$y = 9e^7 - 2.31e^8x + 2.37e^8x^2 - 1.3e^8x^3 + 3.97e^7x^4 - 6e^6x^5 + 442111x^6$	95%

By using Microsoft Excel, the 1<sup>st</sup> order of Polynomial until 6<sup>th</sup> order of Polynomial expression has been generated. Thus, by changing the value of constant's parameter of the expression, will get the model that as close as the simulated return loss result. Based on the data in Table 11 above, the result that showed more accuracy is in 6<sup>th</sup> polynomial order. It gives 95% of accuracy. In order to obtained the modeling, the accuracy of the modeling must be higher that 90%. There are 7 parameters that need to be considered in the 6<sup>th</sup> order polynomial. In order to achieve a good model, the fewer parameters to be considered, the better the model.

## 4.2 Cylindrical Dielectric Resonator Antenna with Coplanar Waveguide Coupling

### 4.2.1 Antenna Structure

Figure 39 below is the cylindrical dielectric resonator antenna (CDRA) with coplanar waveguide feeding technique. The material for the dielectric resonator antenna (DRA) is CCTO ( $\text{CaCu}_3\text{Ti}_4\text{O}_{12}$ ) with  $\epsilon_r=55$  (dielectric constant). The radius of the DRA is 7.2mm, that makes its diameter is 14.4mm. Meanwhile the thickness of the DRA is 3mm. A layer of aluminum is patched on top the DRA and the thickness of the aluminum is 0.05mm. The feeder and the ground plane are made from copper and lossy metal. The purpose of selecting the copper and lossy metal as material because it has the ability to minimize power dissipation, improve reliability, good conductor and affordable.

The width and length of the ground plane is designed to have 50mm and 80mm respectively with its thickness is 1mm. The ground plane uses Rogers RO4003 (lossy) as material at the front surface while at the back the material used is copper. Rogers RO4003 (lossy) dielectric constant is approximately equal to 1 at 2.45 GHz frequency which means the dielectric tolerance and loss can be ignored [31]. The feeder width and length is designed to be 3.8mm and 64.8mm respectively while the DRA is positioned approximately at 41.35mm from the bottom.

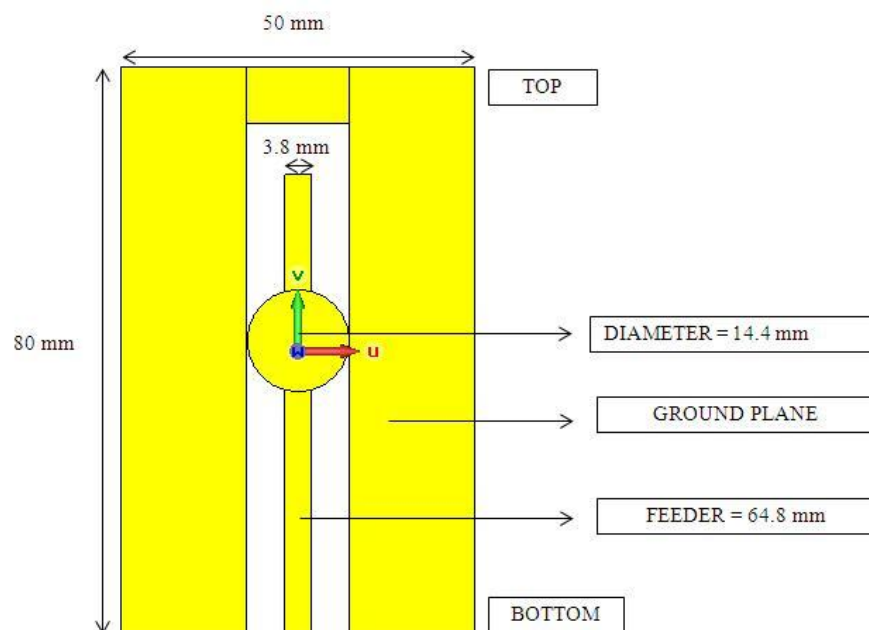


Figure 39 : Front view of the DRA with coplanar waveguide feeding using CST

#### 4.2.1.1 Result of the CDRA with Coplanar Waveguide coupling

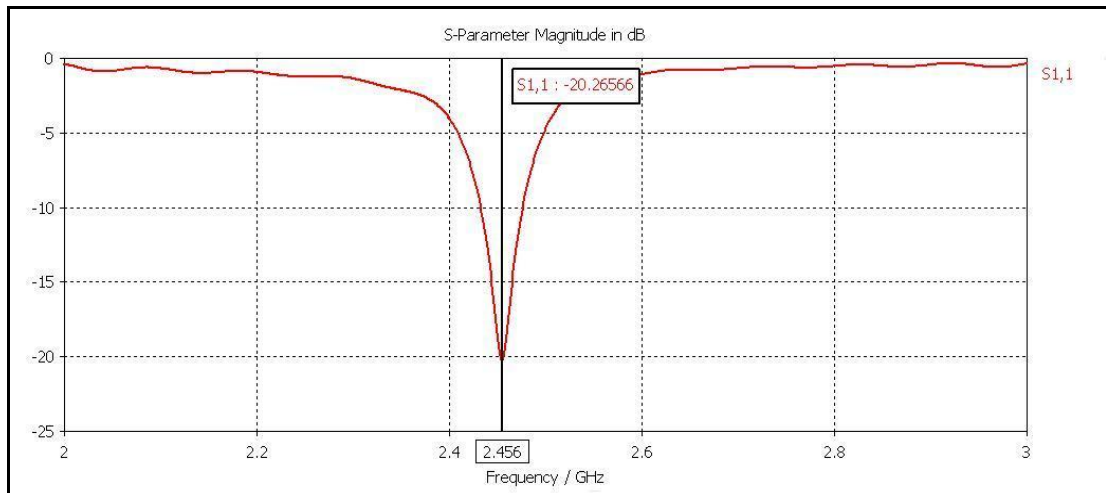


Figure 40 : Return loss of the CDRA

In Figure 40 above shows the simulated result of return loss of the CDRA with microstrip coupling. After obtain the return loss's result of the CDRA with microstrip coupling, all the data have been taken to be recorded.

This antenna achieves a return loss of -20.26566 dB at resonant frequency 2.456 GHz. The simulated return loss value is still acceptable because it is still lower than -10dB. -10 dB is the reference value for an antenna to starts transmits the signal. The gain simulated for the CDRA is 4.531 dB at resonant frequency 2.45GHz. Refer Figure 41 for further information about the result of the gain. The radiation efficiency for the CDRA is -1.699 dB while the total efficiency of the DRA is -1.763 dB. Figure 42 show the directivity of the CDRA is 6.050 dBi. The directivity value must be above 5 dBi in order to make it good antenna.

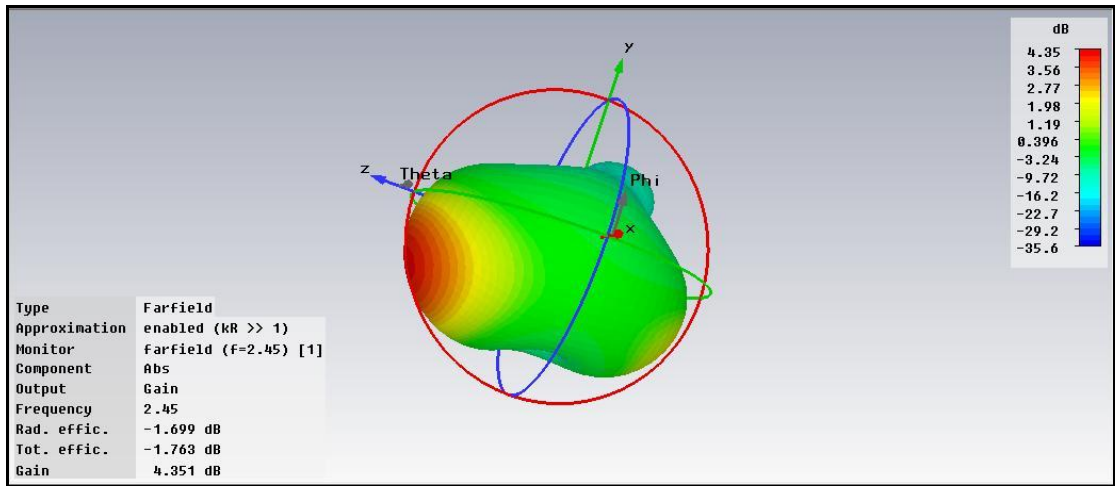


Figure 41 : Gain of the CDRA

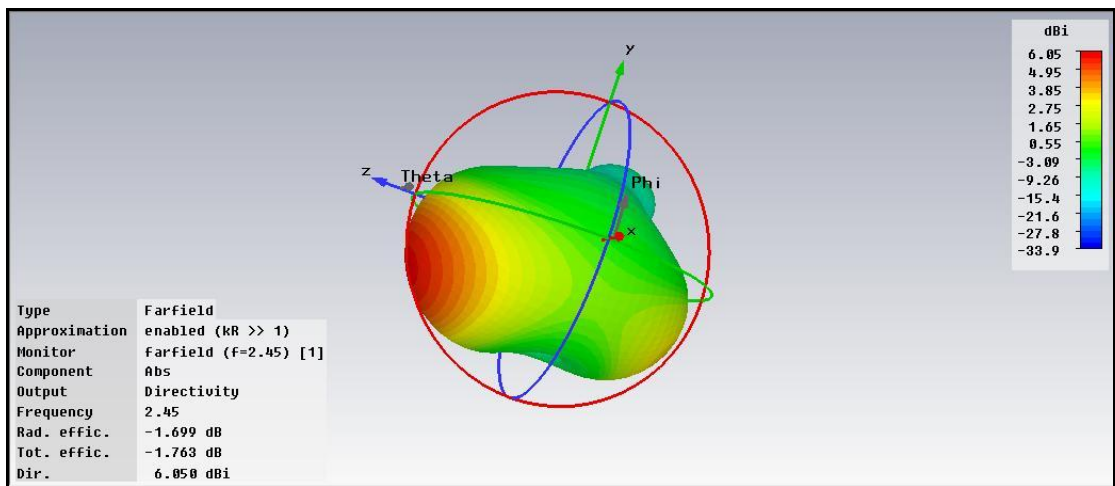


Figure 42 : Directivity of the CDRA

There is also a relationship between the resonant frequencies and the position of the DRA along feed in term of return loss. In this case, the DRA moved along the feed by 1 mm horizontally. Initially, the DRA placed at 39 mm from bottom. Then, simulation took place. After the simulation finished, the DRA moved up by +1 mm vertically until the DRA placed at 42 mm. refer Figure 43, below for further information.

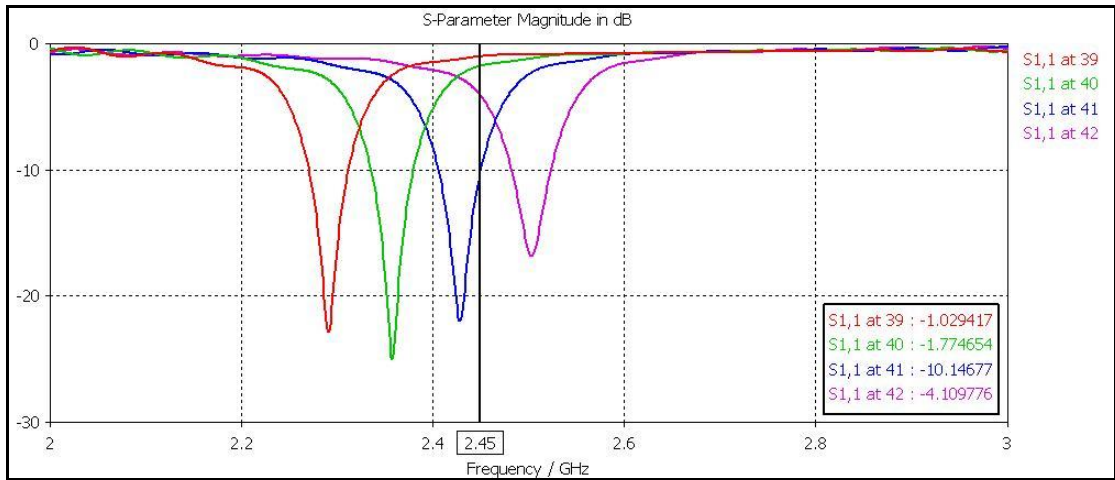


Figure 43 : Return loss when the CDRA positioned from 39 mm to 42 mm from top

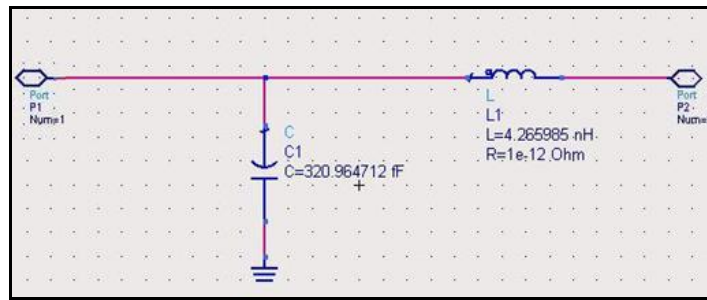


Figure 44 : The equivalent circuit when slot at 39 mm from top

The position of the DRA at 39 mm until 42 mm, it covered from 2.3 GHz up to 2.5 GHz. Based on observation from Figure 43, as for resonant frequency, the higher the position of DRA from bottom, the higher the resonant frequency will be diverted. As for return loss, when the position of the DRA is place at the center of the ground plane in which in this case at 40 mm from top, it will gives better return loss. Refer to Table 12 for further information

Table 12 : Results of Simulated Return Loss at 2.45 GHz

Position of CDRA	Simulated Return Loss at 2.45 GHz
39 mm from top	- 1.029417 dB
40 mm from top	-1.774654 dB
41 mm from top	-10.14677 dB
42 mm from top	-4.109776 dB

As in Figure 44, the equivalent circuit of the coplanar waveguide is constructed referring to the results of return loss obtained. All the equivalent circuit above will be connected to the  $50 \Omega$  resistor in parallel. The circuit represents the frequency tuning capability of the coplanar and it has its own impedance matching. If the value of the capacitance,  $C$  is adjusted, it will affect the return loss. And if the value of the inductance,  $L$  is adjusted, it will affect the value of the resonant frequency.

Refer Table 13 for the recorded data. A plotted graph has been obtained by using all the recorded data from Table 12 by using Microsoft Excel. Please refer Figure 45 to see the plotted graph.

Table 13 : Recorded data from the return loss of the CDRA

Resonant Frequency GHz	S1,1 dB
2.2	-0.9681
2.21	-1.0642
2.22	-1.1581
2.23	-1.2255
2.24	-1.2536
2.25	-1.2467
2.26	-1.2245
2.27	-1.2141
2.28	-1.2398
2.29	-1.3158
2.3	-1.4422
2.31	-1.6054
2.32	-1.7822
2.33	-1.9489
2.34	-2.0937
2.35	-2.2262
2.36	-2.3811
2.37	-2.6127

2.38	-2.9879
2.39	-3.5826
2.4	-4.4867
2.41	-5.8209
2.42	-7.7779
2.43	-10.7255
2.44	-15.4511
2.45	-20.7221
2.46	-15.4016
2.47	-10.5956
2.48	-7.5709
2.49	-5.5384
2.5	-4.1303
2.51	-3.1555
2.52	-2.4968
2.53	-2.0697
2.54	-1.8046
2.55	-1.6403
2.56	-1.5245
2.57	-1.4182
2.58	-1.3007
2.59	-1.1709
2.6	-1.0413
2.61	-0.9297
2.62	-0.8504
2.63	-0.8087
2.64	-0.7992
2.65	-0.8079
2.66	-0.8165
2.67	-0.8092
2.68	-0.778
2.69	-0.7264
2.7	-0.6667

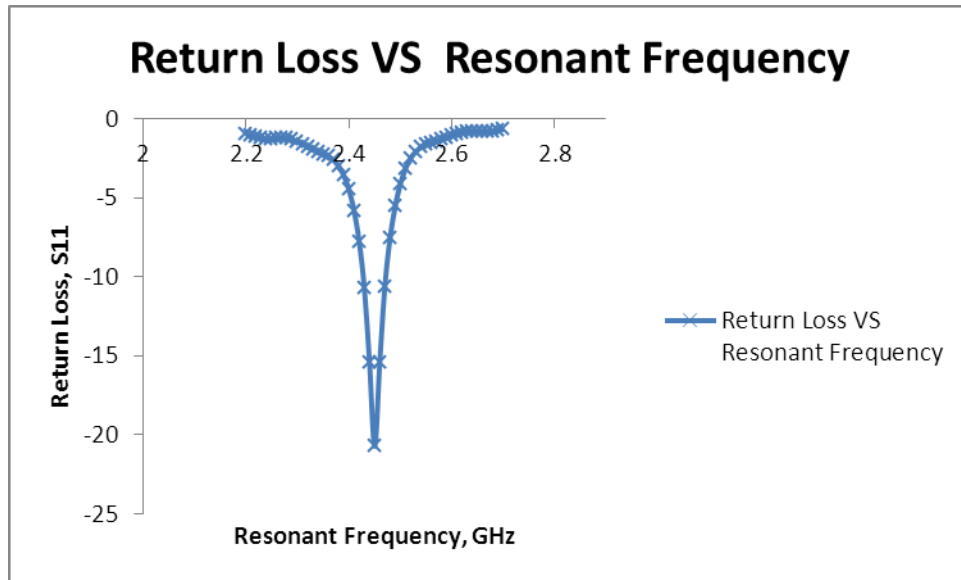


Figure 45 : Plotted graph of CDRA by using Microsoft Excel

From the plotted graphs above, the mathematical equation can be obtained. Thus, the mathematical modeling equation of CDRA using coplanar waveguide coupling has been obtained by using curve fitting method. The general equation of polynomial expression has been generated by using Microsoft Excel based on the plotted graph. The 6<sup>th</sup> order polynomial equation appears as result of modeling. By altering the parameter's constant of the 6<sup>th</sup> order polynomial expression to get the model as close as possible to the original simulated return loss result. Below is the mathematical modeling equation of CDRA using coplanar waveguide coupling.

$$y = 304114x^6 - 4.5e^6x^5 + 2.37e^7x^4 - 8.9e^8x^3 + 1.6e^8x^2 - 1.6e^8x + 6.5e^7 \quad (19)$$

Where;

$$P_1 = 304114$$

$$P_2 = -4.5e^6$$

$$P_3 = 2.73e^7$$

$$P_4 = -8.9e^8$$

$$P_5 = 1.6e^8$$

$$P_6 = -1.6e^8$$

$$P_7 = 6.5e^7$$



Table 14 : Analysis of modeling for Coplanar Waveguide

Polynomial Order	Model	Accuracy Result, %
1 <sup>st</sup> order	$y = -6.32 - 1.23x$	11%
2 <sup>nd</sup> order	$y = 7.25e^2 - 6e^2x + 1.22e^2x^2$	29%
3 <sup>rd</sup> order	$y = 1.24e^3 - 1.24e^3x + 3.8e^2x^2 - 3.55ex^3$	45%
4 <sup>th</sup> order	$y = -2.12e^5 + 3.5e^5x - 2.15e^5x^2 + 5.9e^4x^3 - 6e^3x^4$	66%
5 <sup>th</sup> order	$y = 2.98e^5 + 5.25e^5x - 3.59e^5x^2 + 1.17e^5x^3 - 1.8e^4x^4 + 9.8e^2x^5$	81%
6 <sup>th</sup> order	$y = 6.5e^7 - 1.6e^8x + 1.6e^8x^2 - 8.9e^7x^3 + 2.37e^7x^4 - 4.5e^6x^5 + 304114x^6$	92%

By using Microsoft Excel, the 1<sup>st</sup> order of Polynomial until 6<sup>th</sup> order of Polynomial expression has been generated. Thus, by changing the value of constant's parameter of the expression, will get the model that as close as result of the simulated return loss. Based on the data in Table 13 above, the result that showed more accuracy is in 6<sup>th</sup> polynomial order. It gives 92% of accuracy. In order to obtained the modeling, the accuracy of the modeling must be higher that 90%. There are 7 parameters that need to be considering in the 6<sup>th</sup> order polynomial. In order to achieve a good model, the fewer parameters to be considered, the better the model.

## **CHAPTER 5**

### **CONCLUSION AND RECOMMENDATIONS**

#### **5.1 Conclusion**

From this project, curve fitting method can be used to obtain the modeling. It can be obtained by using the result of the return loss simulation. Based on that, the graph can be plotted. By using the plotted graph, the curve fitting method will be used to generate the general equation of polynomial expression. Based on the polynomial expression, the value of the parameters will be altered in order to obtain the model that as close as the result of the simulated return loss. The 6<sup>th</sup> order polynomial has been chosen to be the model since it produces very accurate result. To obtain a good modeling, the accuracy of the model must be higher than 90% compared to the original result. The exponential smoothing cannot be implemented in this project because the graph of the return loss from the simulation produced a polynomial graph.

Instead of modeling, different coupling method will produce different performance of antenna. In this project, the microstrip coupling gives a good return loss result.

Lastly, hope the model developed will help the engineers and designers to design and gain understand about antenna since there is rapid development of wireless microwave system that demands on high-performance, low power consumption communication units particularly for portable devices.

#### **5.2 Recommendation**

For future works, in order to model a good antenna, the modeling itself should produce a simple mathematical equation. It is because, if a lot of parameter that need to be considered, it will be hard for designers to control all the parameters at a time. If

possible, by using curve fitting method, try to get the model to fit in 2<sup>nd</sup> or 3<sup>rd</sup> order of polynomial because they provide less parameter that to be considered.

In order to produce a good antenna, the return loss of the antenna must be below than -10 dB. So as for improvement, try to get the antenna to produce return loss at -50 dB since the results of the return loss of the simulation in this project is within the range of 20 to 35 dB. But also have to make sure that the antenna can be operated at 2.45 GHz. The directivity of the antenna also must be more than 5 dBi as the input impedance is typically design for 50  $\Omega$ . And also, try to use other method of coupling to DRA in order to see the performance of the DRA. There are other method to coupling to DRA such as probe coupling and dielectric image guide coupling method. Also, try to use other shape of DRA instead of using cylindrical. There are other shapes of DRA such as split cylindrical, hemispherical and rectangular DRA.

## REFERENCES

- [1] Richtinger, R.D., "Dielectric Resonators," *Journal of Applied Physics*, June 1939, Vol. 10, pp 391-398.
- [2] Petosa, A., A. Ittipiboon, "Dielectric Resonator Antenna: A Historical Review and the Current State of the Art", *IEEE Antennas and Propagation Magazine*, Vol. 52, No. 5, October 2010.
- [3] Okaya, A., and L.F. Barash., "The Dielectric Microwave Resonator," *Proceedings of the IRE*, Vol 50, October 1962., pp 2,081-2,092.
- [4] Denidni, T. A., Y. Coulibaly, and L. Talbi., "Design of a broadband hybrid dielectric resonator antenna for x-band applications," *J. of Electromagn. Waves and Appls.*, Vol 20, No 12, 1629-1642, 2006.
- [5] Yang, R., Y. -J. Xie, P. Wang, and L. Li., "Microstrip antennas with left-handed materials substrates," *J. of Electromagn. Waves and Appl.*, Vol. 20, No 9, 1221-1233, 2006.
- [6] Tadjalli, A., A. R. Sebak, and T. A. Denidni., " Resonance frequencies and far field patterns of elliptical dielectric resonator antenna: analytical approach," *Progress In Electromagnetics Research*, PIER 64, 81-98, 2006.
- [7] Bujimon, P. V., S. K. Menon, M. N. Suma, M. T. Sebastian, and P. Mohanan., "Broadband cylindrical dielectric resonator antenna excited by modified microstrip line," *Electronics Letters*, Vol 41, Issue 7, 385-387, March 31, 2005.
- [8] Xiao, J. -K., S. -P. Li, and Y. Li., "Novel planar bandpass filters using one single patch resonators with corner cuts," *J. of Electromagn. Waves and Appl.*, Vol 20, No. 11, 1481-1493, 2006.
- [9] wikipedia. *wikipedia*. [Online] [http://en.wikipedia.org/wiki/Mathematical\\_model](http://en.wikipedia.org/wiki/Mathematical_model).
- [10] P. Wade, N1BWT, and M.Riley, KB1VC., "Metal Lens Antennas for 10 GHz," *Proceedings of the 18th Eastern VHF/UHF Conference*, ARRL, May 1992, pp. 71-78.
- [11] John Kraus, *Antennas*, McGraw Hill, 1956.
- [12] Silver, Samuel. *Microwave Antenna Theory and Design*. s.l. : McGraw Hill, 1949. Vol. 12 of Radiation Laboratory Series, reprinted 1984.
- [13] Haneishi, M., and H. Takazawa, "Broadband Circularly Polarised Planar Array Composed of a Pair of Dielectric Resonator Antennas," *IEE Electronics Letters*, Vol.21, No.10, May 1985, pp.437 - 438
- [14] Birand, M. T., and R. V. Gelsthorpe, "Experimental Millimetric Array Using Dielectric Radiators Fed by Means of Dielectric Waveguide," *IEE Electronics Letters*, Vol. 17, No.18, Sept. 1981, pp. 633 - 635.
- [15] Cohn, S. B., "Microwave Bandpass Filters Containing High Q Dielectric Resonators," *IEEE Transactions on Microwave Theory & Techniques*, Vol. 16, April 1968, p 218-227.

- [16] Huang, Kao-Cheng and Edwards, David J., "Millimetre wave antennas for gigabit wireless communications: a practical guide to design and analysis in a system context," *USA: John Wiley & Sons*, 2008.
- [17] Leung, K. W., et al., "On the TM<sub>101</sub> Mode of Dielectric Resonator Antenna," *Microwave Optical Technology Letters*, Vol 6, No. 11, Sept. 1993, pp 626-629.
- [18] Mongia, R. K., and P. Bhartia., "Dielectric Resonator Antennas-A Review and General Design Relations for Resonant Frequency and Bandwidth," *International Journal of Microwave and Millimeter-Wave Computer-Aided Engineering*, Vol 4, No. 3, 1994, pp 230-247.
- [19] Kishk, A. A., A. W. Glisson, and G. P. Junker., "Study of Broadband Dielectric Resonator Antennas," *1999 Antenna Applications Symposium*, Allerton Park, Monticello, IL, pp 45-68.
- [20] Simons, R.N., and R.Q. Lee, "Effect of Parasitic Dielectric Resonators on CPW/Aperture-Coupled Dielectric Resonator Antennas," *IEE Proceedings Part-II*, Vol. 140, Oct. 1993, pp 336 – 338.
- [21] Leung, K.W., et al., "Annular-Slot Coupled Dielectric Resonator Antenna," *IEE Electronics Letters*, Vol 34, No. 13 June 1998, pp. 1,275-1,277.
- [22] Huang, C. Y., J. Y. Wu, and K. L. Wong, "Cross-Slot-Coupled Microstrip Antenna and Dielectric Resonator Antenna for Circular Polarization," *IEEE Transactions on Antennas & Propagation*, Vol. 47, No. 4, April 1999, pp. 605-609.
- [23] Leung, K.W., and K.K. So, "Rectangular Waveguide Excitation of Dielectric Resonator Antenna," *IEEE Transaction on Antennas & Propagation*, Vol. 51, No. 9, Sept 2003, pp. 2,477- 2,481.
- [24] Long, S.A., McAllister, and L.C. Shen, "The Resonant Cylindrical Dielectric Cavity Antenna," *IEEE Transaction on Antennas & Propagation*, Vol. 31, No. 3, March 1983, pp. 406-412.
- [25] Chen, Z.N., et al., "Effect on Parasitic Disk on a Coaxial Probe-Fed Dielectric Resonator Antenna," *Microwave and Optical Technology Letters*, Vol. 15, No. 3, June 1997, pp. 166-168.
- [26] Cooper, M., et al., " Investigation of Dielectric Resonator Antennas for L-Band Communications," *Symposium on Antenna Technology and Applied Electromagnetics ANTEM 96*, Montreal, Canada, Aug. 1996, pp. 167-170.
- [27] Leung, K.W., K.M. Luk, and K.Y.A. Lai, " Input Impedance of a Hemispherical Dielectric Resonator Antenna," *IEE Electronics Letters*, Vol.27, No. 24, Nov. 1991, pp. 2,259-2,260.
- [28] Kranenburg, R.A., S.A. Long, "Microstrip Transmission Line Excitation of Dielectric Resonator Antennas," *IEE Electronics Letters*, Vol. 24, No. 18, Sept. 1998, pp. 1,156-1,157.
- [29] A. A. Kishk, A. Ittipiboon, Y. M. M. Antar, M. Cuhaci, "Dielectric Resonator Antenna Fed by a Slot in the Ground Plane of a Microstrip Line", *Proc. Eight Int. Conf. on Antennas and Propagation, ICAP'93*, Apr. 1993, Part 1, pp.540 – 543.

[30] S. M. Shum and K. M. Luk, "Stacked Annular Ring Dielectric Resonator Antenna Excited by Axi-Symmetric Coaxial Probe", *IEEE Transactions on Antennas and Propagation*, Vol 43, August 199, pp. 889 – 892.

[31] ROGERS CORPORATION, RO4000 Laminates – Datasheet, "Advanced Circuit Materials RO4000 Series High Frequency Circuit Materials," Publication #92-004.

